NASA TECHNICAL NOTE

NASA TN D-4893

NASA TN D-4893

ANALYSIS OF COMMUTATED NETWORKS EMPLOYING FEEDBACK CIRCUITS

by Michael T. Borelli

George C. Marshall Space Flight Center
Huntsville, Ala.

NATIONAL AERONAUTICS AND SPACE ADMINISTRATION • WASHINGTON, D. C. • NOVEMBER 1968

NASA TN D-4893

ANALYSIS OF COMMUTATED NETWORKS EMPLOYING FEEDBACK CIRCUITS

By Michael T. Borelli

George C. Marshall Space Flight Center
Huntsville, Ala.

NATIONAL AERONAUTICS AND SPACE ADMINISTRATION

For sale by the Clearinghouse for Federal Scientific and Technical Information
Springfield, Virginia 22151 – CFSTI price $3.00

TABLE OF CONTENTS

TABLE OF CONTENTS (Concluded)

LIST OF ILLUSTRATIONS

LIST OF ILLUSTRATIONS (Continued)

LIST OF ILLUSTRATIONS (Concluded)

LIST OF TABLES

DEFINITION OF SYMBOLS

Symbol	Definition
a, b, c, d	transmission matrix elements
A	equal to $\left(\frac{N\alpha}{\tau s + 1}\right)$; a constant
b	dead time
B	equal to $\left[2\tau\omega_0 \tanh \frac{\pi}{2} \left(\frac{\tau s + 1}{\tau \omega_0}\right)\right] \Big/ [\pi(\tau s + 1)]$
C	capacitor; equal to $(\tau s + 1 - j2kN\tau\omega_0)$
e	voltage as a function of time
E	voltage as a function of frequency
F	transfer function
G	transfer function
H	transfer function
i, k, ℓ, m, n, r	indices
k, K	a constant
$\mathcal{L}$	Laplace transform operation
n	order of harmonics
N	a constant
p	a commutation function
q	a commutation function
R	resistor; resistor matrix
s	Laplace operator

DEFINITION OF SYMBOLS (Concluded)

Symbol	Definition
t	time
t_d	time delay
T	period
u, v, x, y, z	variables as a function of time
U, V, X, Y, Z	variables as a function of frequency
Z	impedance
$\propto$	gain constant
γ	constant
ϕ	phase angle
τ	time constant
ω	frequency
ω_0	commutation frequency
ω_c	break-frequency
$\circledast$	convolution
Subscripts	
i, n, 0, ij	indices
i	input variable
0	output variable
n	order of harmonics

ANALYSIS OF COMMUTATED NETWORKS EMPLOYING FEEDBACK CIRCUITS

INTRODUCTION

The development of advanced automatic control systems often requires new and unusual circuits, components, techniques, and other such items, to provide the necessary control to accomplish a specific mission. An adaptive automatic flight control system for large space booster vehicles has been developed [1-4] that uses tracking-notch filters composed of commutated networks (CN's). From this successful application and others cited in the literature, it appears that these networks are particularly well suited for use in tracking filters.

A commutated network is an electrical network, either active or passive, consisting of resistors and reactive elements which are switched or commutated in some periodic manner. In this investigation of CN's and in most practical cases, the reactive elements are capacitors. The commutation action in a resistor-capacitor CN can transform the frequency response characteristics of a low-pass filter into that of a highly selective band-pass filter. Effective low-frequency band-pass or band-elimination filters can be realized without the use of magnetic elements. These and other transformations of a network's basic characteristics provide very interesting properties that are useful for some special applications. The CN's are also called chopper networks [5] or modulation-demodulation networks [6] for full-wave balanced chopping or modulating circuits. When the frequency of the input signal to the network is the same as the commutation frequency, the networks are called synchronous networks [7].

Two simple mechanizations of CN's are shown in Figures 1 and 2. The network of Figure 1 consists of two commutators with capacitors connected to corresponding commutator elements. The two commutator elements of each capacitor undergo simultaneous commutation by a pair of wipers or brushes driven at a specific frequency of rotation. The commutation action of this CN is referred to as balanced half-wave commutation and is discussed briefly later in this report. This CN, or a similar configuration, has been analyzed by Le Page [8], Smith [9], Fischl [10], and others. The network of Figure 2 represents the more practical circuit and it can be mechanized with either

electromechanical relays or electronic switches. The commutation action of this CN is called full-wave balanced commutation and it is the commutation used in this investigation. Multicapacitor networks with polyphase commutation functions can be obtained easily by interconnecting networks of this type and other basic CN's. The analysis techniques applicable to the network of Figure 2 can be extended to apply to the network of Figure 1, as shown by Franks and Sandberg [11].

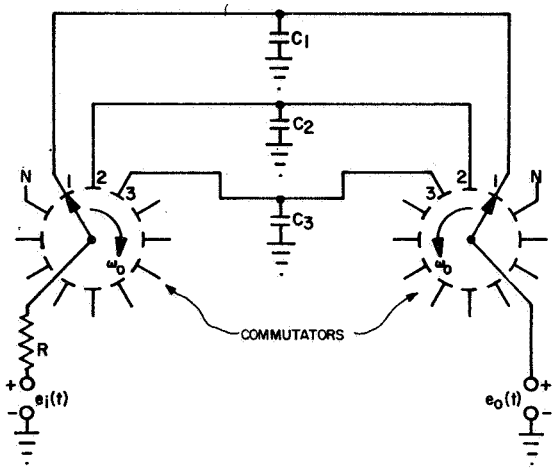

FIGURE 1. AN N-CAPACITOR CN

A number of real problems involving the tracking of a signal frequency have generated a considerable amount of literature on CN's. Most papers dealing with analysis are usually restricted to a particular network configuration and the restraints imposed limit the application of the results. Some investigators have attempted to generalize the results of their work; for example, Franks and Sandberg [11] presented an excellent analysis of polyphase CN's which they called an N-path filter. Tobin [12] made an extensive study of synchronous networks which are a subclass of CN's and consequently do not reveal some important CN characteristics. The analysis of CN's starts with either the single-capacitor unit or with an N-capacitor unit, where N is assumed extremely large. The single-capacitor CN can be analyzed easily using differential equations or difference equations. Neither of these methods, however, can be extended readily to apply to polyphase CN's. Operational methods are usually employed when treating polyphase CN's. The restraint imposed by assuming a large number of capacitors in the CN is usually employed to justify the use of sample-data theory; the dwell time is extremely short when compared to the total period. If this assumption is invalid and if sample-data techniques

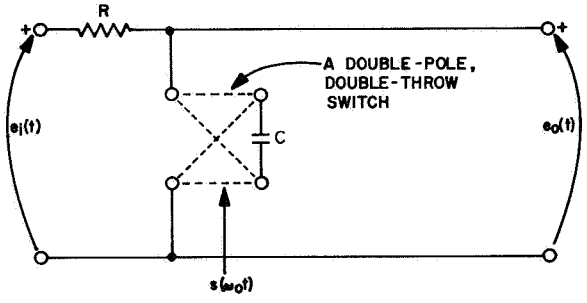

FIGURE 2. A SINGLE-CAPACITOR CN

are used, then finite-width sampling analysis would have to be used with its attendant complexity.

In the literature reviewed, a good, accurate frequency domain analysis of the single-capacitor CN was missing. Therefore, an analytical and experimental investigation was undertaken to fill this void. Some very basic relationships of single-capacitor and multicapacitor CN's were revealed in this study. Transient analysis of CN's has been treated by Tobin [12], Asner [13], and Feaster [14] and does not constitute a part of this investigation.

The analysis of CN's with a feedback path, although a very real problem, has not received much attention in the literature. In AC carrier control systems, where modulation introduces undesirable harmonics in the control loop, it is almost universally assumed that a low-pass filter in the system's output circuit suppresses all the harmonics, and therefore only the input signal frequency is considered present in the feedback path. Carroll [15] treated the problem of CN's with constant gain elements in the feedback path and included the effects of all the harmonics generated by the commutation action. A new method for analyzing CN's with frequency dependent elements in the feedback path, which represents a generalization of Carroll's work and an extension of Frank's and Sandberg's work, is developed later in this report.

Because experimental data are used to substantiate analytical results, a detailed description of the experimental procedures is given in Appendix A.

METHODS OF ANALYSIS

The methods of analysis briefly described here are those employing full-wave balanced commutation and include:

1. Classical Method
2. Difference Equations
3. Modulation Equivalents
4. Laplace Transforms.

Before proceeding with the discussion of these techniques, the difference between full-wave and half-wave balanced commutation functions will be examined. The terms commutation or switching will usually be used in place of the terms modulation, demodulation, or chopping, as might be found in the indicated literature references. Unbalanced commutation will not be treated in this investigation and therefore all future references to commutation, unless otherwise stated, are to balanced commutation.

Commutation Functions

The type of commutation function used in this investigation is called an ideal square wave function and can be expressed mathematically in several ways. For illustration purposes, the commutation function can be written as

$$p(t) = \frac{\sin \omega_0 t}{|\sin \omega_0 t|}, \tag{1}$$

where ω_0 is the commutation frequency in radians per second. The function $p(t)$ has an amplitude of ± 1 and a period T equal to $2\pi/\omega_0$ seconds. The commutation function $p(t)$ is the analytical expression of the square wave switching function $s(\omega_0 t)$ and is shown as a function of time in Figure 3. As seen in Figure 3, $p(t)$ is a quasi-continuous function and is defined over the entire interval T.

For mathematical convenience, the expression for $p(t)$ used later in this report is the complex Fourier series of the ideal square-wave, or

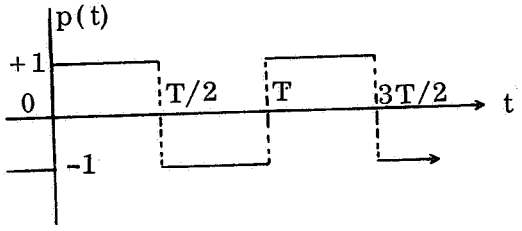

FIGURE 3. IDEAL FULL-WAVE COMMUTATION FUNCTION

$$p(t) = \sum_{\substack{n=-\infty \\ \text{odd}}}^{+\infty} \frac{-2j}{n\pi} \epsilon^{jn\omega_0 t}. \tag{2}$$

The Fourier series representation of $p(t)$ satisfies the criterion $p(t) \cdot p(t) = 1$ everywhere, except at a countable number of points, i.e., at $t = \frac{kT}{2}$ where $k = 0, \pm 1, \pm 2, \pm 3 \ldots$ and the function is always finite. Frequent use will be made of powers of $p(t)$, such as $[p(t)]^2 = 1$, $[p(t)]^3 = p(t)$, etc.

A half-wave commutation function $r(t)$ is shown in Figure 4. The complex Fourier series for the function in Figure 4 is

$$r(t) = \frac{1}{2} - \sum_{\substack{n=-\infty \\ \text{odd}}}^{+\infty} \frac{j}{n\pi} \epsilon^{jn\omega_0 t} . \tag{3}$$

This is the function that applies to the CN of Figure 1 for the two-capacitor case. A number of techniques have been used to analyze CN's employing half-wave commutation. Fischl [10] used time-varying transforms, Franks and Sandberg [11] used Laplace transforms, and Tou [16] used point by point methods. Although the analytical techniques developed here are for CN's employing full-wave commutation, they are also applicable to CN's employing half-wave commutation.

It is known that ideal full-wave commutation cannot be obtained in real circuits. There is always some dead-time where the value of $p(t)$ is neither + 1 or - 1, as shown in Figure 5. The Fourier series for the function of Figure 5 is

$$p(t) = \sum_{\substack{n=-\infty \\ \text{odd}}}^{+\infty} \frac{-2j}{\pi n} \cos\left(\pi n \frac{2b}{T}\right) \epsilon^{jn\omega_0 t} , \tag{4}$$

where 2b is the dead-time.

As b approaches zero, in equation (4), the nonideal commutation approaches the ideal commutation case. Tobin [12], Asner [13], and Wilson [5] have treated CN's with nonideal commutation. The case of full-wave nonsymmetrical commutation functions has been investigated by Borelli and Hosenthien [1] and by Asner [13].

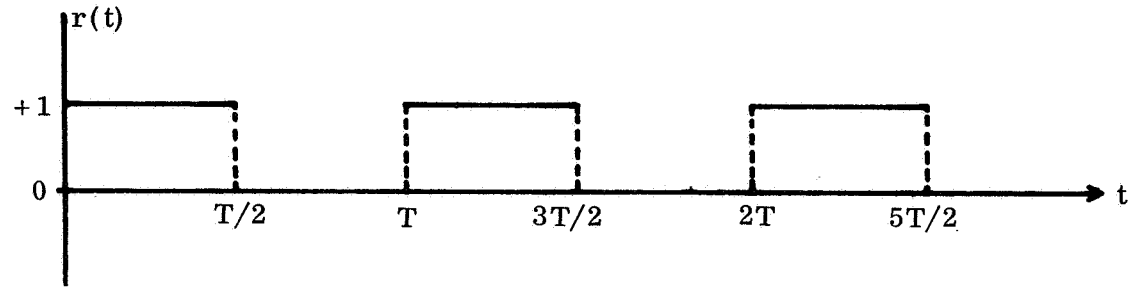

FIGURE 4. HALF-WAVE COMMUTATION FUNCTION

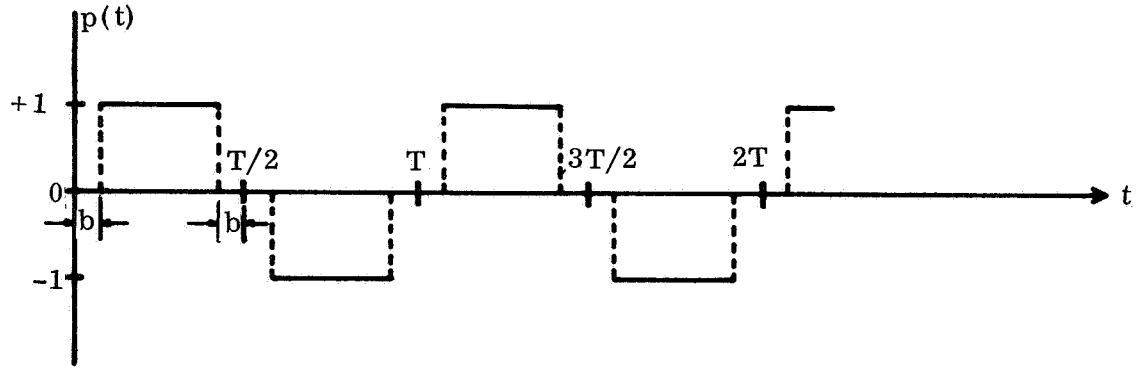

FIGURE 5. NONIDEAL FULL-WAVE COMMUTATION FUNCTION

The effects of nonideal commutation can be ignored in practically all servo-control applications when modern electronic switching techniques are employed for commutation. A commutation circuit developed by McGowan [4] has a switching time on the order of ten microseconds (10×10^{-6}). For a 400 Hz carrier control system, the cosine term in equation (4) would be

$$\cos\left(2\pi n \frac{5 \times 10^{-6}}{1/400}\right) = \cos\left(2\pi n \times 0.002\right),$$

and for the fundamental term, or $n = 1$, this term would be $0.9992 \approx 1$. Thus, the dead-time is negligible. The effects of nonideal commutation will not be investigated further.

Methods of Analysis

A basic active CN that will be used repeatedly in this investigation is shown in Figure 6. The reason for selecting the active two-terminal-pair CN is that a considerable number of experimental studies have been made using this particular network configuration. The operational amplifier itself will be assumed linear and will not be analyzed in detail because it is not a necessary part of the commutated network. The operational amplifier is used to provide an added degree of flexibility.

The dynamical equation for the circuit of Figure 6 can be shown to be [1]

$$\frac{d(py)}{dt} + \frac{1}{\tau} py = \frac{\alpha}{\tau} px \tag{5}$$

where

$y = y(t)$, the output voltage

$x \mp x(t)$, the input voltage

$p = p(t) = s(\omega_0 t)$, the commutation function

$\alpha = -\frac{R_1}{R_0}$

$\tau = R_1 C$.

Equation (5) is a linear differential equation with time varying coefficients and there are several ways of solving it.

The classical method of solution used by Roan [17] is the simplest of the four methods being reviewed in this section. However, for polyphase CN's, that is, if more than one commutation function is employed in the network, the complexity of the analysis problem increases very rapidly. Because the commutation function being employed has a value of either + 1 or - 1, equation (5) can be solved by substituting into the equation the appropriate value of p(t) for

a specific period of time and then specifying an input for x(t). Roan used a sinusoidal input signal and zero initial conditions. Equation (5) was then solved repetitively and an expression for the output, y(t), for any interval of time was derived. Roan did not extend his analysis to polyphase CN's.

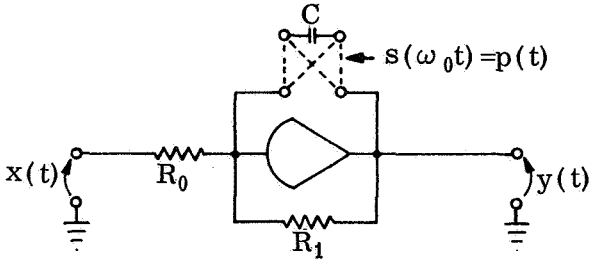

FIGURE 6. A SINGLE-CAPACITOR CN

The classical method was also used by Asner [13] to analyze a CN employing two commutation functions having a relative time delay of T/4 seconds, as shown in Figure 7. The specific CN analyzed is shown in Figure 8.

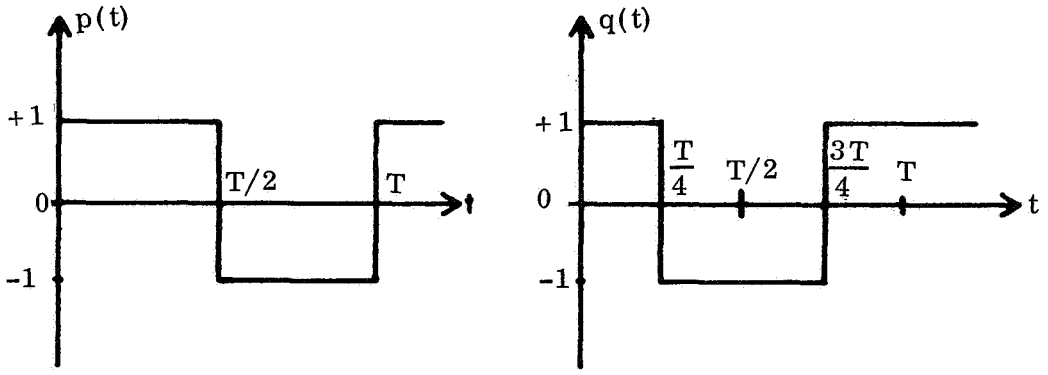

FIGURE 7. COMMUTATING FUNCTIONS

The dynamical equation representing the CN of Figure 8 was converted into two linearly independent differential equations with time varying coefficients. For some n^{th} period of commutation, where n is any positive integer, an initial condition was assumed and the input signal was specified as a sinusoidal voltage. The two differential equations were solved for each quarter of the n^{th} commutation period. The actual value of the initial condition was obtained for each quarter-period by using a linear difference equation, and the resulting expression is very similar to that derived by Roan. With the solution for each quarter-period of commutation and the initial condition to match the boundary conditions, Asner obtained a solution in the time domain.

Difference equation methods were used by Tobin [12] to generate both the transient and steady-state responses for a generalized single-capacitor synchronous network. A synchronous network, a special case of the CN, was

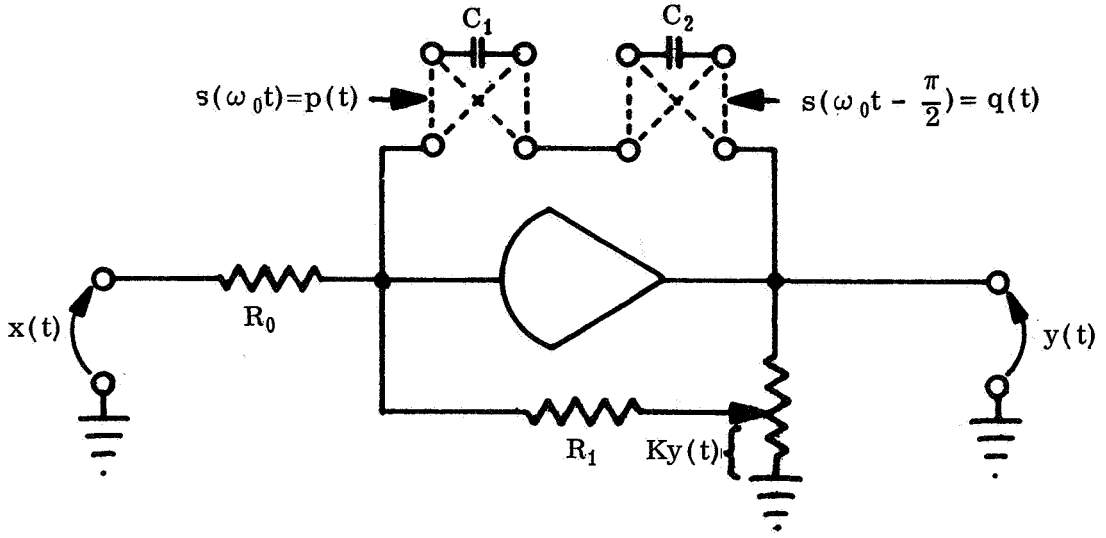

FIGURE 8. A TWO-CAPACITOR CN

previously defined. The analysis consisted of solving the two circuit voltage equations, in difference equation form, for the charge on the capacitor at the beginning of each switching interval of time resulting from the commutation action. The charge on the capacitor at the beginning of each switching interval is the initial condition for that interval. With the two circuit voltage equations and the initial condition, a continuous solution was obtained between each switching interval. Tobin extended his results to handle polyphase synchronous networks but the method becomes very complex in much the same manner as the classical method.

The method of modulation equivalents was developed by Hosenthien [18] to analyze AC circuits employing suppressed-carrier amplitude modulation. The method consists of resolving the network's input and output signals into an orthogonal set, with reference to the fundamental frequency component of the square wave commutation function. Thus, the component of the input signal in phase with the fundamental frequency component of the commutation function would constitute the direct component; the component of the input signal either delayed or advanced by T/4 seconds with respect to the fundamental frequency component of the commutation function would constitute the quadrature component. The Laplace transform complex translation theorem [19] is used to derive a two-by-two transfer matrix from the noncommutated transfer function of the CN. Using Laplace transforms and matrix algebra, the system can be analyzed and the output can be expressed in terms of the derived transfer

matrix and the Laplace transform of the input signal. As special cases, the CN's of Figures 6 and 8 can be analyzed by the method of modulation equivalents with a single frequency input signal. The method will also handle the analysis of polyphase CN's [20].

The Laplace transform method was applied to the analysis of the N-path filter by Franks and Sandberg [11]. The particular configuration analyzed is shown in Figure 9. By redrawing the CN of Figure 1, an equivalence to the N-path filter configuration can easily be visualized with the proper selection of the commutation functions $p_N(t)$. However, the correspondence between the N-path filter of Figure 9 and the CN of Figure 10 is not quite so readily discernible. Later it will be shown that the equivalent block diagram of the CN of Figure 10 is the configuration of Figure 9.

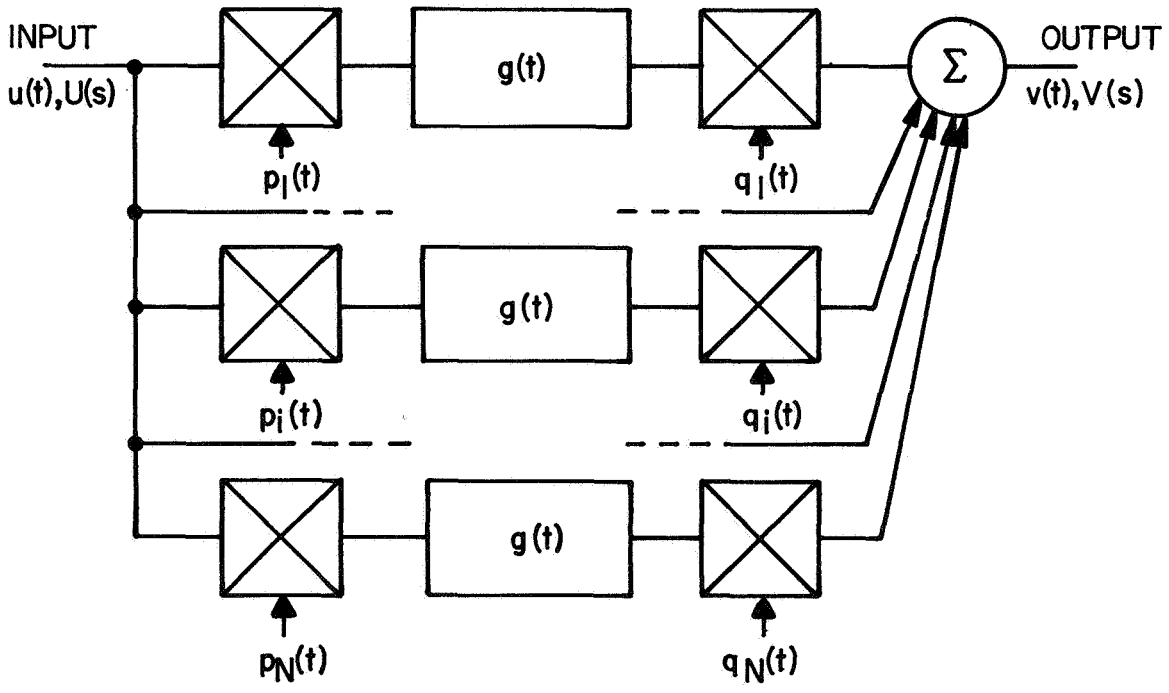

FIGURE 9. THE N-PATH FILTER

The expressions derived by Franks and Sandberg to characterize the network of Figure 9 are

$$V(s) = \sum_{k=-\infty}^{+\infty} F(k, s)\, U(s - jkN\omega_0) \tag{6}$$

$$F(k, s) = N \sum_{\ell=-\infty}^{+\infty} Q_\ell P_{kN-\ell} G(s - j\ell\omega_0) \tag{7}$$

where N is the number of forward paths in the network and $P_{kN-\ell}$ and Q_ℓ are the coefficients of the complex Fourier series of the commutating functions. In the CN's analyzed here, the commutation functions p(t) and q(t), as shown in Figure 9, are identical.

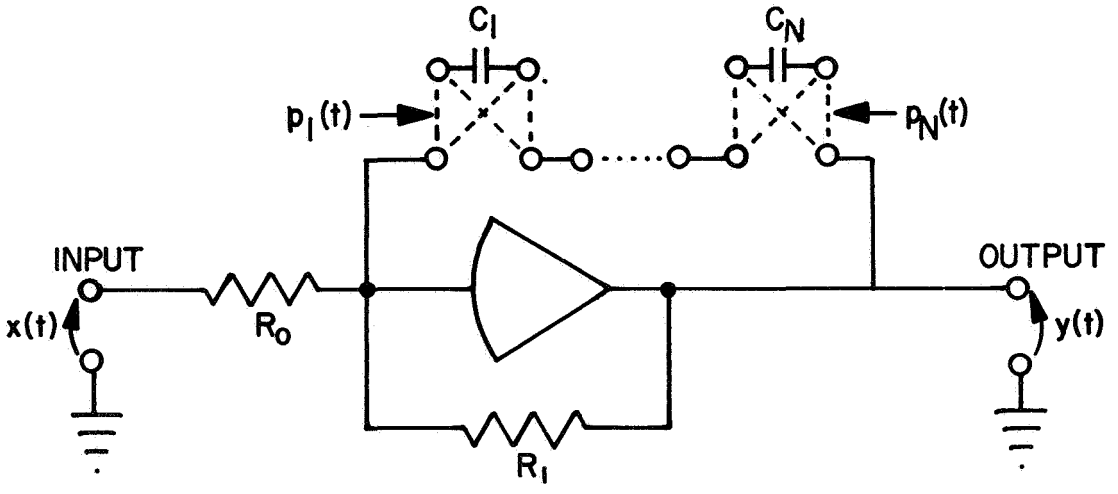

FIGURE 10. AN N-CAPACITOR CN

Franks and Sandberg used a complete period of commutation to determine the phasing of their commutation functions, while in other sources [1-4] and in this paper, a half-period of commutation is used for phasing the commutation functions. The half-period phasing gives the same results, except for a gain factor proportional to the number of commutation functions, as the full-period phasing but with only half the number of commutated elements. The Laplace transform method briefly discussed here is used for the analysis of CN's throughout the remaining sections.

This brief review of several different methods for handling the analysis of CN's does not indicate a clear superiority for any particular method. As is usually the case, the problem to be solved dictates the best method of solution. For example, the analysis of the N-path filter is best accomplished by the Laplace transform method of Franks and Sandberg, whereas the analysis of a system using suppressed carrier amplitude modulation would probably be easier using the modulation equivalence method or the difference equation method. The Laplace transform method has been extended to solve a wider range of problems than any of the other methods. For example, the polyphase CN with a feedback element was solved for a particular network configuration by Carroll [15] and is generalized in this paper using the Laplace transform method, whereas none of the other methods have been extended to obtain the exact solution to this type of problem.

Definition of Terms

Linearity of Commutated Networks. The CN's analyzed in this investigation exhibit both linear and nonlinear characteristics. They have linear properties in that they are composed of linear passive elements and any associated amplifiers are maintained in their linear range of operation. The superposition theorem applies to CN's as it does to noncommutated linear networks. Equation (5) can be used to show how the superposition theorem applies to a CN.

Let $y_1(t)$ be a solution to equation (5) for an applied signal $x_1(t)$, or

$$\frac{d(py_1)}{dt} + \frac{1}{\tau} p\, y_1 = \frac{\alpha}{\tau} p\, x_1 , \tag{8}$$

and let y_2 also be a solution to equation (5) for an applied signal x_2, or

$$\frac{d(py_2)}{dt} + \frac{1}{\tau} p\, y_2 = \frac{\alpha}{\tau} p\, x_2 \tag{9}$$

where x, y, p, α, and τ are defined for equation (5).

For superposition to hold, it must be shown that $y_3 = y_1 + y_2$ is also a solution of equation (5) for an input of $x_3 = x_1 + x_2$. Adding equations (8) and (9) yields

$$\frac{dp(y_1 + y_2)}{dt} + \frac{1}{\tau} p(y_1 + y_2) = \frac{\alpha}{\tau} p(x_1 + x_2), \tag{10}$$

since α, τ, and p are independent of y and x. The solution $y_3 = y_1 + y_2$ is the required solution for an input of $x_3 = x_1 + x_2$; therefore, superposition applies.

The nonlinear property of CN's is the generation of an infinite number of signal components, at different frequencies, that appear in the output signal of the CN. The generation of these signal components results from the commutation or modulation (multiplying) action of the input signal with the square-wave commutation function. A description of these signal components is given in the next section.

Output Signal Frequencies of a CN. The output signal of a CN is theoretically composed of an infinite number of signal components with different frequencies, as can be seen by examination of equation (6). Each of the infinite number of signal frequencies appearing in the output of the CN has a definite frequency relation to some even order harmonics of the commutation frequency, ω_0. The even order harmonics depend upon the number of commutation functions employed in the CN and their relative phasing. For example, if equation (6) is applicable to a specific CN with N = 4, the even harmonics under discussion would be at $4\omega_0$, $8\omega_0$, $12\omega_0$, and so forth. The frequencies of the components appearing in the output signal would be at $(4\omega_0 \pm \omega)$, $(8\omega_0 \pm \omega)$, $(12\omega_0 \pm \omega)$, and so forth, where ω is the input signal frequency. In a frequency spectrum, these output signal components are located symmetrically above and below the even harmonics of the commutation frequency; therefore, they will be called "side-band" frequencies of the commutation signal.

If the input signal frequency is equal to an integral multiple of the commutation function frequency, then the output signal components will be at frequencies that are harmonics of the commutation frequency, ω_0. If the input signal frequency is an odd multiple of ω_0, the output harmonics will be of odd orders; if the input signal frequency is an even multiple of ω_0, the output harmonics will be of even orders. The output signal components of a CN will therefore be composed of either harmonics or side-band frequencies of the commutation frequency, ω_0, plus a component at the input signal frequency.

Phase. There are two basic phase relations to be considered in a single-capacitor CN. One is the usual phase relation that exists between the input and output signals of any network [21]. However, since the output signal of a CN is

composed of an infinite number of components at different frequencies, the output signal component used to specify this phase relation will be that component having the same frequency as the input signal.

The second phase relation to be discussed is the phase between the input signal and the commutation function. The CN input signal in this investigation will always be used as the reference signal and will therefore have zero phase shift. When the input signal frequency is equal to the commutation frequency ω_0, the phase between the two signals at any time can be defined as

$$\phi = -t_d\omega_0 \tag{11}$$

where t_d is the time delay of the commutation function as shown in Figure 11. This phase relation ϕ can be incorporated in the mathematical expression of the commutation function p(t) as

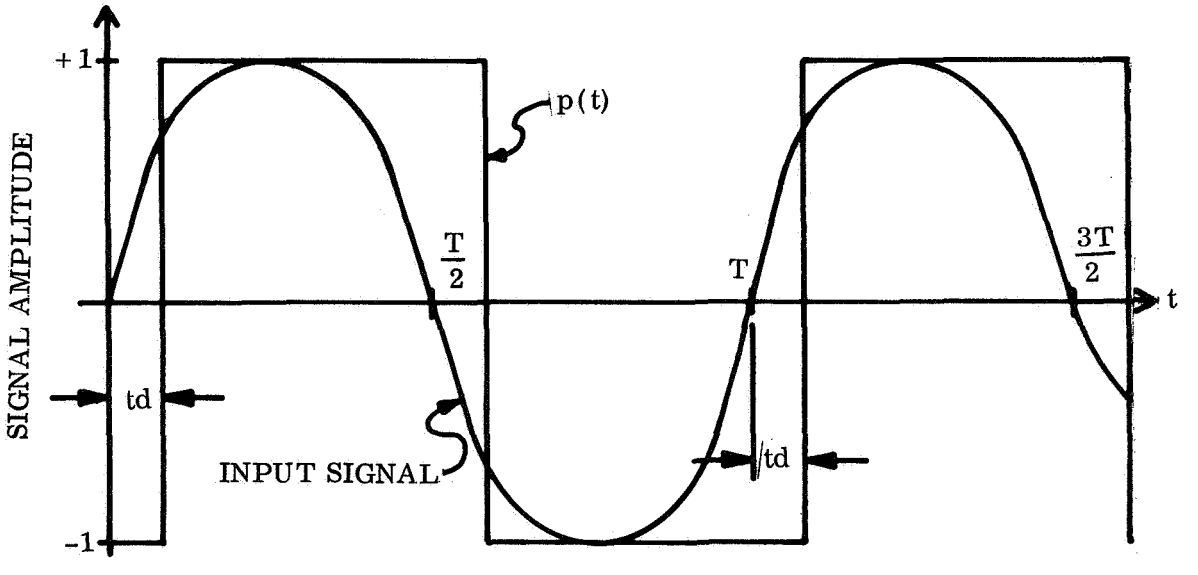

FIGURE 11. TIME DELAY BETWEEN INPUT SIGNAL AND COMMUTATION FUNCTION

$$p(t) = \sum_{n=-\infty}^{+\infty} \frac{-2j}{n\pi} \epsilon^{jn\omega_0(t+\frac{\phi}{\omega_0})}$$

where ϕ is defined in equation (11).

SINGLE-PHASE RC COMMUTATED NETWORKS

General

An RC commutated network can be constructed in many different ways, but from the practical point of view, there are only three linear circuit configurations of primary importance. They are: (1) the passive one-terminal-pair network, (2) the passive two-terminal-pair network, and (3) the active two-terminal-pair network. These three configurations for the single-capacitor case are shown in Figures 12, 13, and 14, respectively. The resistor networks shown in Figures 12 and 13 are perfectly general but are restricted to linear resistors. The resistor network associated with the operational amplifier of Figure 14 is constrained only to maintain the amplifier in the nonsaturated region of operation. The switching or commutation function $s(\omega_0 t)$ is the same for all three circuits and is considered to be a perfect switching function; that is, it has zero dead-time, and the dwell periods in both positions are of equal duration.

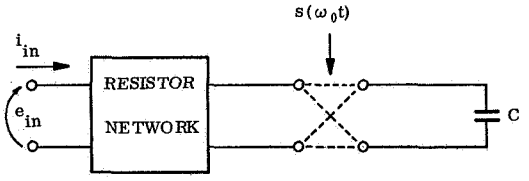

FIGURE 12. PASSIVE ONE-TERMINAL-PAIR CN

In this section three essential points are considered:

1. The derivation of the CN equivalent block diagram
2. The analysis of single-capacitor CN's
3. The effect of the CN parameters on its operating characteristics.

The manner in which the three basic CN's will be treated is shown in the analysis flow diagram of Figure 15. The analysis of polyphase CN's and

the subject matter of the last block in Figure 15, "Feedback Analysis Problem," will be treated later in this report.

Equivalent Block Diagram

For the analysis of the single-capacitor case, the active two-terminal-pair CN of Figure 14 will be used. The techniques used in the analysis of this network are also applicable to the analysis of the networks of Figures 12 and 13, the passive one-terminal- and two-terminal-pair networks.

Laplace transform techniques will be used in this analysis, but first an equivalent block diagram applicable to any single-capacitor CN will be derived that will materially aid in the analysis to follow. The CN of Figure 16 is shown as a generalized single-capacitor CN in Figure 14 and the following theorem is used to obtain its equivalent block diagram, shown in Figure 17.

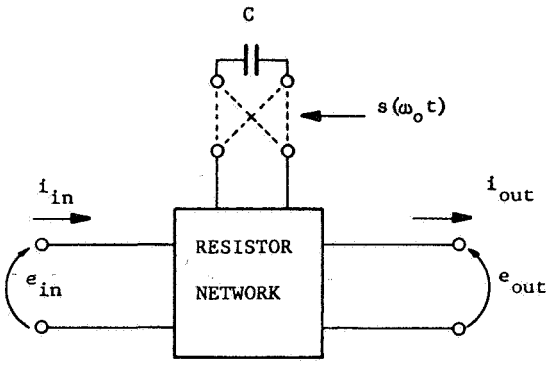

FIGURE 13. PASSIVE TWO-TERMINAL-PAIR CN

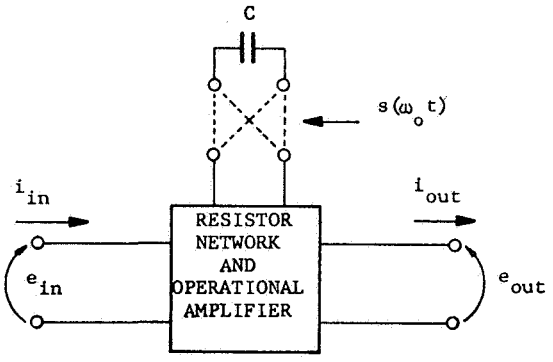

FIGURE 14. ACTIVE TWO-TERMINAL-PAIR CN

Theorem I

If a linear CN consists of resistors R_m ($m = 1, 2, \ldots, M$) and a single capacitor C_1, and if the capacitor is being commutated perfectly at a frequency ω_0, then the CN can be represented by an equivalent block diagram consisting of a modulator, a network, and a demodulator, all connected in cascade, where the modulator and demodulator are driven by a perfect square-wave function of frequency ω_0 and where the network has the same transfer function as the CN with the exception that the commutated element is now non-commutated.

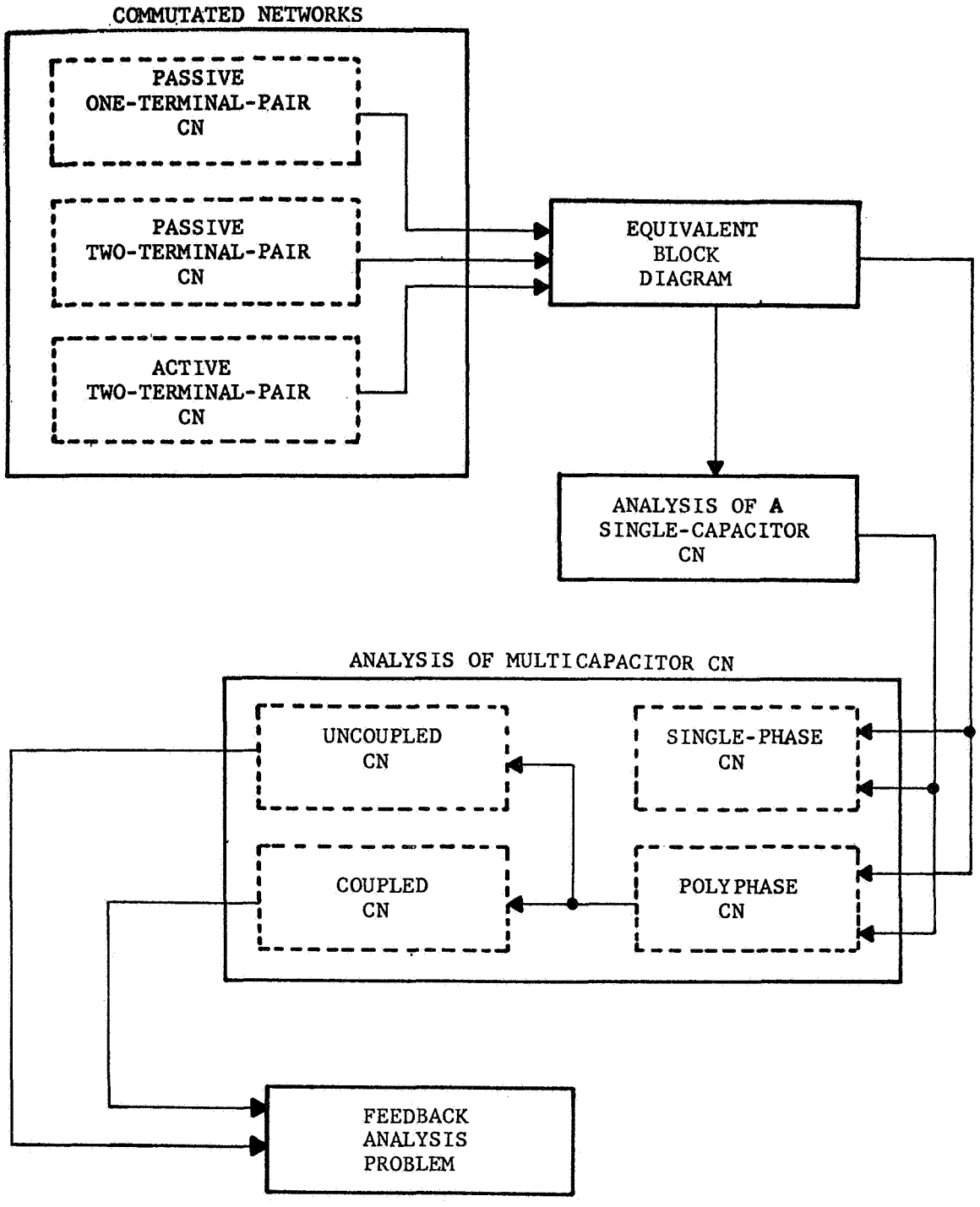

FIGURE 15. ANALYSIS FLOW DIAGRAM OF RC COMMUTATED NETWORKS

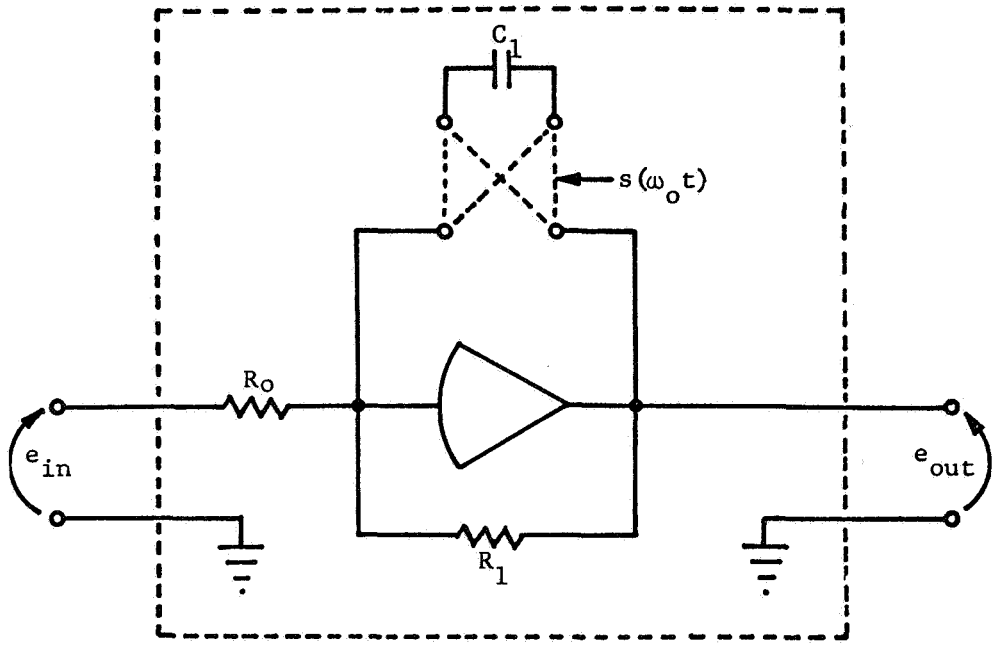

FIGURE 16. ACTIVE SINGLE-CAPACITOR CN

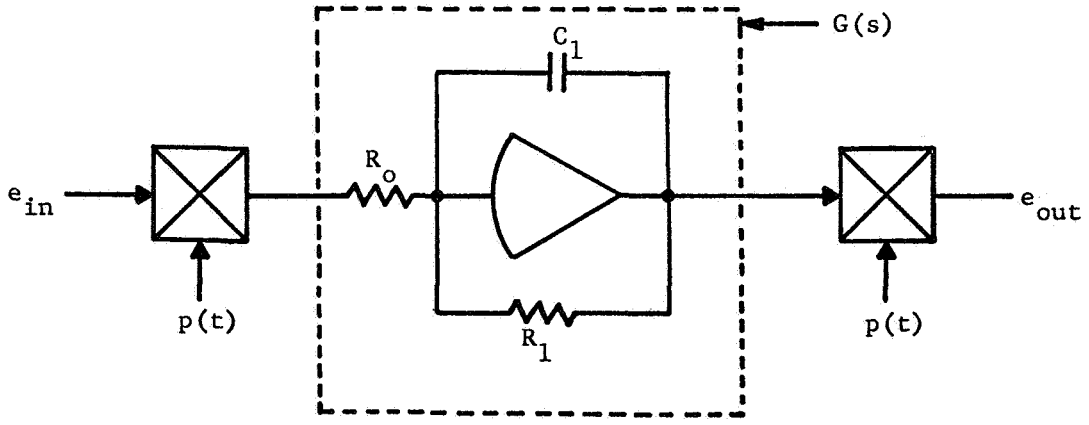

FIGURE 17. AN EQUIVALENT BLOCK DIAGRAM OF THE SINGLE-CAPACITOR CN OF FIGURE 16

It should be noted that Theorem I applies to active as well as passive CN's and to one-terminal-pair networks as well as two-terminal-pair networks. We will define G(s) as the ratio of the Laplace transform of the output variable

to the Laplace transform of the input variable of the noncommutated network in the s domain. When the CN is a one-terminal-pair network, then G(s) is a driving-point immittance function; when the CN is a two-terminal-pair network, G(s) is a transfer function. The term "linear commutated network" means that the superposition theorem holds for this network. The output of the CN will, of course, contain an infinite number of either harmonics or sideband frequency signals as well as the input signal frequency. The modulating function p(t) of Figure 17 is the analytical expression of the square-wave switching function $s(\omega_0 t)$ and is shown as a function of time in Figure 3. Theorem I will be proven first for one-terminal-pair single-capacitor CN's and then for two-terminal-pair single-capacitor CN's. The proof for the one-terminal-pair CN will consist of two steps:

1. The terminal characteristics of a commutated single-capacitor RC network are shown to be invariant to the location of the resistor network with respect to the switch when the network is undergoing perfect commutation.

2. Simple commutation or switching action is shown to be representable by modulation and demodulation.

The term "simple commutation" means a single commutator or switch. Higher order switching, where switches are connected in cascade, sometimes with intervening networks, will be discussed later is this section.

Step 1 is illustrated in Figure 18, where the resistor network R is perfectly general. To show that circuit I is equivalent to circuit II, two-terminal-pair matrix algebra will be used. The equations for circuit I during the positive half-period, when connections a-a′ exist for both circuits, are

$$\begin{pmatrix} E_i \\ I_i \end{pmatrix} = \begin{pmatrix} a & b \\ c & d \end{pmatrix}\begin{pmatrix} 1 & 0 \\ 0 & 1 \end{pmatrix}\begin{pmatrix} 1 & 0 \\ sC & 1 \end{pmatrix}\begin{pmatrix} E_0 \\ -I_0 \end{pmatrix} = \begin{pmatrix} a + bCs & b \\ c + dCs & d \end{pmatrix}\begin{pmatrix} E_0 \\ -I_0 \end{pmatrix}, \quad (13)$$

where the terms a, b, c, and d are the elements of the transmission matrix of the resistor network and the identity matrix is the transmission matrix for the switch during the positive half-period of the commutation period. For circuit II the equations are

$$\begin{pmatrix} E_i \\ I_i \end{pmatrix} = \begin{pmatrix} 1 & 0 \\ 0 & 1 \end{pmatrix}\begin{pmatrix} a & b \\ c & d \end{pmatrix}\begin{pmatrix} 1 & 0 \\ sC & 1 \end{pmatrix}\begin{pmatrix} E_0 \\ -I_0 \end{pmatrix} = \begin{pmatrix} a + bCs & b \\ c + dCs & d \end{pmatrix}\begin{pmatrix} E_0 \\ -I_0 \end{pmatrix}. \quad (14)$$

The equations for circuit I during the negative half-period of $s(\omega_0 t)$, when connections b-b′ are in effect, are

$$\begin{pmatrix} E_i \\ I_i \end{pmatrix} = \begin{pmatrix} a & b \\ c & d \end{pmatrix}\begin{pmatrix} -1 & 0 \\ 0 & -1 \end{pmatrix}\begin{pmatrix} 1 & 0 \\ sC & 1 \end{pmatrix}\begin{pmatrix} E_0 \\ -I_0 \end{pmatrix} = -\begin{pmatrix} a + bCs & b \\ c + dCs & d \end{pmatrix}\begin{pmatrix} E_0 \\ -I_0 \end{pmatrix}, \quad (15)$$

and for circuit II,

$$\begin{pmatrix} E_i \\ I_i \end{pmatrix} = \begin{pmatrix} -1 & 0 \\ 0 & -1 \end{pmatrix}\begin{pmatrix} a & b \\ c & d \end{pmatrix}\begin{pmatrix} 1 & 0 \\ sC & 1 \end{pmatrix}\begin{pmatrix} E_0 \\ -I_0 \end{pmatrix} = -\begin{pmatrix} a + bCs & b \\ c + dCs & d \end{pmatrix}\begin{pmatrix} E_0 \\ -I_0 \end{pmatrix}. \quad (16)$$

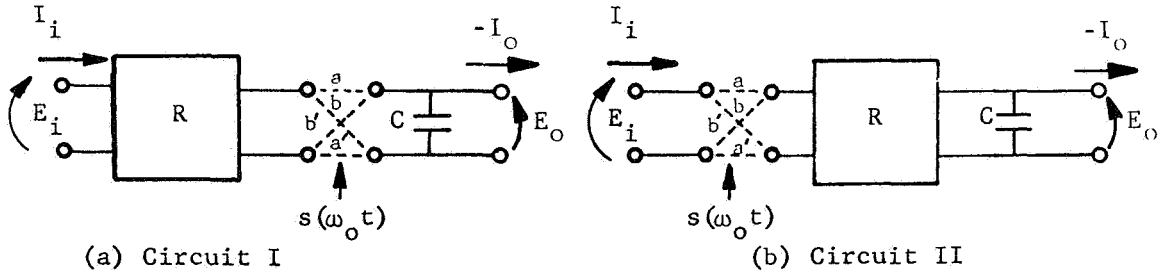

(a) Circuit I (b) Circuit II

FIGURE 18. EQUIVALENT TWO-TERMINAL-PAIR CN'S

The solutions of equations (13) and (14) for the positive half-period of commutation will be the same for the same initial voltage on C and the solutions of equations (15) and (16) for the negative half-period of commutation will be the same for the same initial conditions. Thus shifting the resistor network to either side of the switch does not affect the terminal characteristics of the network.

Step 2 can be shown easily with the aid of Figure 19, again letting the switching function $s(\omega_0 t)$ remain equal to $p(t)$. Also, let $g\{i'(t)\}$ denote a linear operation on $i'(t)$. Then the equations for the circuit of Figure 19 are

$$i'(t) = p(t) \cdot i(t) \quad (17)$$

$$e'(t) = p(t) \cdot e(t) \tag{18}$$

$$e'(t) = g\{i'(t)\} \tag{19}$$

$$p(t) \cdot e(t) = g\{i'(t)\} = g\{p(t) \cdot i(t)\} \tag{20}$$

or

$$e(t) = p(t) \cdot g\{p(t) \cdot i(t)\} \tag{21}$$

since $p(t) \cdot p(t) = 1$.

A block diagram representation of equation (21) is shown in Figure 20, where $x(t) = i(t)$, $y(t) = e(t)$, and $q(t) = p(t)$. In this case the first multiplier represents a modulator and the second multiplier represents a demodulator. In Figure 20, the function G(s) is a driving-point immittance function for a single-capacitor one-terminal-pair CN.

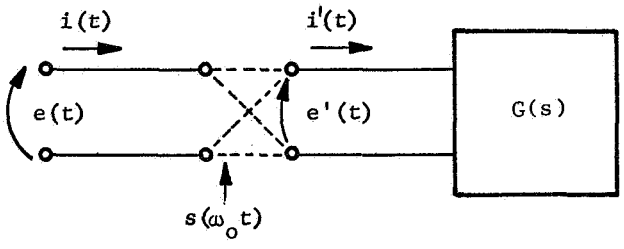

FIGURE 19. A GENERALIZED ONE-TERMINAL-PAIR CN

To prove Theorem I for the two-terminal-pair single-capacitor CN, it will be necessary only to show that the single switch shown in Figure 21(a) can be replaced by two switches as shown in Figure 21(b) where R represents a resistor network, either with or without an ideal operational amplifier. The equivalent block diagram of Figure 20 is recognized as the single-line diagram of Figure 21(b). To complete the proof of Theorem I, it is necessary only to show that the diagram of Figure 21(b) is equivalent to the diagram of Figure 21(a). To show this, the following lemma will be used:

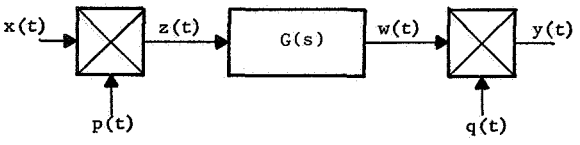

FIGURE 20. A GENERALIZED EQUIVALENT BLOCK DIAGRAM OF A CN

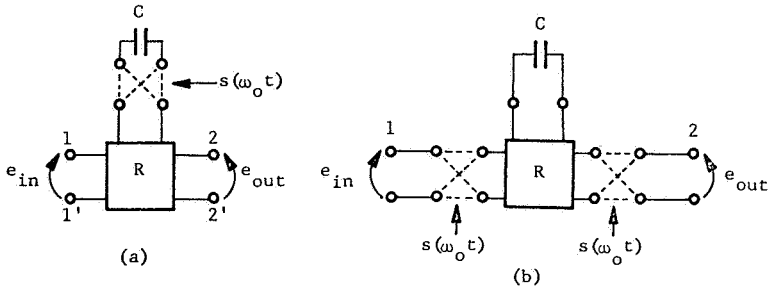

FIGURE 21. EQUIVALENT ONE-CAPACITOR, TWO-TERMINAL-PAIR CN'S

Lemma I. 1

> If R represents a resistive N-terminal-pair CN consisting of linear time-invariant elements, and if all commutation functions of the network are perfect and in phase with each other, then the terminal characteristics between any two terminal pairs will behave like a noncommutated network if there is an even number of commutations existing between the two terminal pairs; otherwise, with an odd number of commutations, the terminal characteristics will behave as if there were one commutation between the two terminal pairs.

The proof of Lemma I. 1 is given as follows: since all the resistors are time-invariant, the voltage between any pair of input terminals and any pair of output terminals can be written as

$$e_i(t) = e_j(t) \cdot k_{ij} \cdot [p(t)]^n \qquad (22)$$

where $e_i(t)$ is the input voltage, $e_j(t)$ is the output voltage, and the value of k_{ij} depends on the resistor network between the input and the output terminals. Since $p(t) \cdot p(t) = 1$ is true, then if n is even, $[p(t)]^n = 1$ results; whereas if n is odd, $[p(t)]^n = p(t)$ results. The proof of Step 1, used in Theorem I, is now used; that is, the proof that a resistor network's terminal characteristics remain invariant in regard to its location with respect to the switch. This completes the proof of Lemma I. 1. A simple illustration of Lemma I. 1 is shown in Figure 22.

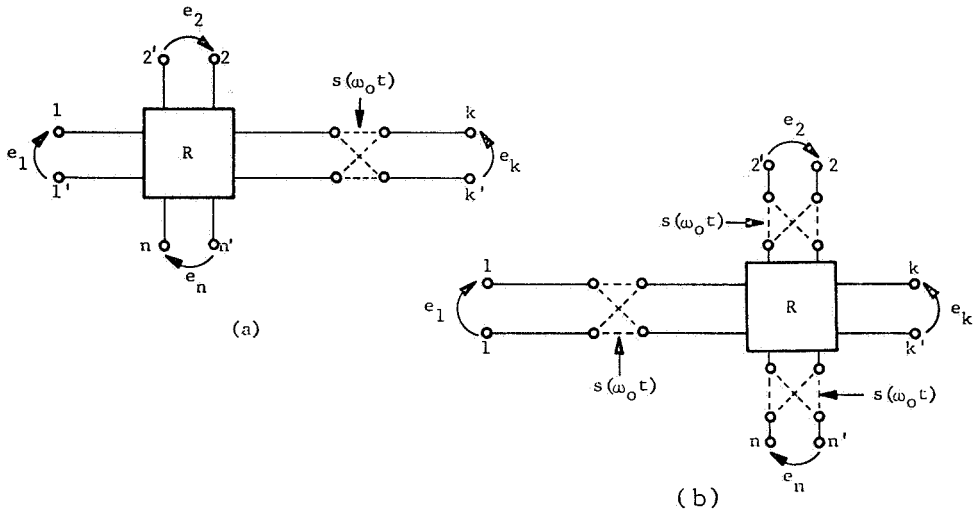

FIGURE 22. EQUIVALENT N-TERMINAL-PAIR CN'S

Using Lemma I. 1, the resistor network R of Figure 21(a) is modified as in Figure 23(a). Again the equations $s(\omega_0 t) = p(t)$ and $p(t) \cdot p(t) = 1$ hold true, so the diagram of Figure 23(a) simplifies to the diagram of Figure 23(b) and the proof of Theorem I is completed.

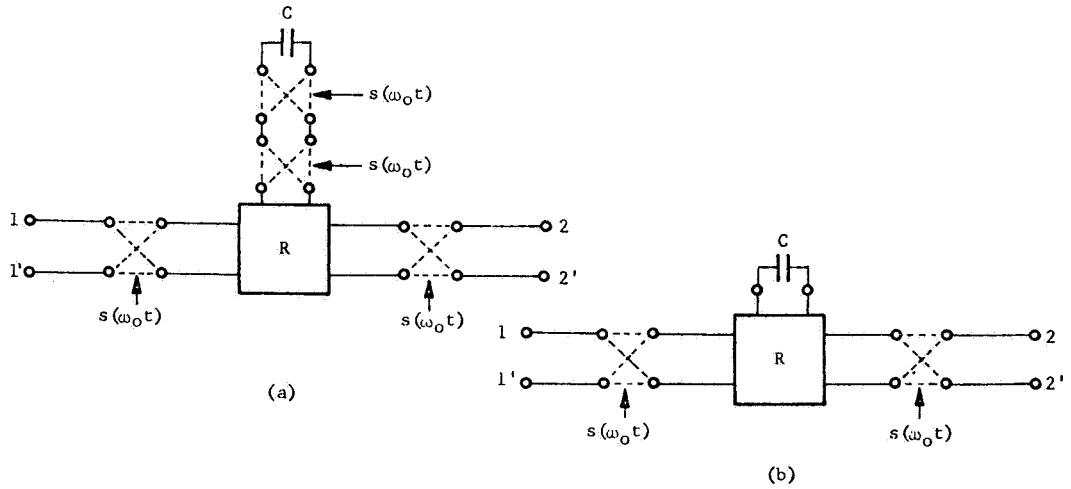

FIGURE 23. EQUIVALENT TWO-TERMINAL-PAIR CN'S

Theorem I can also be applied to multicapacitor CN's to obtain the corresponding equivalent block diagram, as will be shown later.

Analysis of a Single-Capacitor CN

The analysis of a single-capacitor CN serves as a basis for the analysis of multicapacitor CN's and reveals some interesting characteristics of a commutated network that might otherwise be obscured if only multicapacitor CN's were analyzed. The equivalent block diagram of a general single-capacitor CN as shown in Figure 20 will be used for this analysis. The output of the modulator is

$$z(t) = x(t) \cdot p(t). \tag{23}$$

The Laplace transform of equation (23) is

$$Z(s) = X(s) \circledast P(s) \tag{24}$$

where $\circledast$ indicates complex convolution. The square-wave commutating function, similar to that shown in Figure 3 except for the phase parameter ϕ, can be written as

$$p(t) = \sum_{\substack{n=-\infty \\ \text{odd}}}^{+\infty} \frac{-2j}{\pi n} \epsilon^{jn\omega_0(t+\frac{\phi}{\omega_0})}, \tag{25}$$

where $-\frac{\phi}{\omega_0}$ is the time delay of the commutation function with respect to the input signal x(t) (Fig. 11). The Laplace transform of equation (25) yields

$$P(s) = \sum_{\substack{n=-\infty \\ \text{odd}}}^{+\infty} \frac{-2j}{\pi n} \frac{\epsilon^{jn\phi}}{s - jn\omega_0}. \tag{26}$$

To distinguish between the modulation and the demodulation functions, the demodulation function is represented by $q(t)$, where

$$q(t) = \sum_{\substack{\ell=-\infty \\ \text{odd}}}^{+\infty} \frac{-2j}{\pi \ell} \epsilon^{j\ell\omega_0(t+\frac{\phi}{\omega_0})} \tag{27}$$

and its Laplace transform is

$$Q(s) = \sum_{\substack{\ell=-\infty \\ \text{odd}}}^{+\infty} \frac{-2j}{\pi \ell} \frac{\epsilon^{j\ell\phi}}{s - j\ell\omega_0} . \tag{28}$$

Substituting equation (26) into equation (24) yields

$$Z(s) = X(s) \circledast \sum_{\substack{n=-\infty \\ \text{odd}}}^{+\infty} \frac{-2j}{\pi n} \frac{\epsilon^{jn\phi}}{s - jn\omega_0} . \tag{29}$$

By using the Laplace transform complex translation theorem, equation (29) becomes

$$Z(s) = \sum_{\substack{n=-\infty \\ \text{odd}}}^{+\infty} \frac{-2j}{\pi n} \epsilon^{jn\phi} X(s - jn\omega_0) . \tag{30}$$

The output of the block diagram of Figure 20 is $y(t)$ and it can be written as

$$y(t) = q(t) \cdot w(t) \tag{31}$$

where

$$w(t) = \mathcal{L}^{-1} \{G(s) Z(s)\} \tag{32}$$

and $G(s)$ can be either a transfer function or a driving-point immittance function.

Taking the Laplace transform of equation (32) gives

$$W(s) = G(s) \cdot Z(s). \tag{33}$$

The Laplace transform of equation (31) is

$$Y(s) = Q(s) \circledast W(s). \tag{34}$$

Substituting equations (28), (30), and (33) into equation (34) yields

$$Y(s) = -\frac{4}{\pi^2} \sum_{\substack{\ell=-\infty \\ \text{odd}}}^{+\infty} \frac{1}{\ell} \frac{\epsilon^{j\ell\phi}}{s - j\ell\omega_0} \circledast G(s) \sum_{\substack{n=-\infty \\ \text{odd}}}^{+\infty} \frac{X(s - jn\omega_0)}{n} \epsilon^{jn\phi}. \tag{35}$$

Using the Laplace transform translation theorem in equation (35) gives

$$Y(s) = -\frac{4}{\pi^2} \sum_{\substack{n=-\infty \\ \text{odd}}}^{+\infty} \frac{1}{n} \sum_{\substack{\ell=-\infty \\ \text{odd}}}^{+\infty} \frac{X(s - j\omega_0[\ell + n])}{\ell} \epsilon^{j\phi(\ell+n)} G(s - j\ell\omega_0). \tag{36}$$

Since ℓ and n are always odd integers, then $\ell + n = 2r$, where $r = 0, \pm 1, \pm 2, \pm 3, \ldots$, and $n = 2r - \ell$. Applying these relations in equation (36), we find that

$$Y(s) = -\frac{4}{\pi^2} \sum_{r=-\infty}^{+\infty} \sum_{\substack{\ell=-\infty \\ \text{odd}}}^{+\infty} \frac{X(s - j2\omega_0 r)}{\ell(2r - \ell)} \epsilon^{j2\phi r} G(s - j\ell\omega_0). \tag{37}$$

Changing the summation on ℓ so that ℓ is summed over only the positive integers, we see that

$$Y(s) = -\frac{4}{\pi^2} \sum_{r=-\infty}^{+\infty} X(s - j2\omega_0 r) \epsilon^{j2\phi r} \sum_{\substack{\ell=1 \\ \text{odd}}}^{+\infty} \left\{ \frac{G(s - j\ell\omega_0)}{\ell(2r - \ell)} - \frac{G(s + j\ell\omega_0)}{\ell(2r + \ell)} \right\}. \tag{38}$$

Equation (38) is the exact expression for the output of the single-capacitor CN of Figures 12, 13, and 14. If the network is a one-terminal-pair network, then G(s) is a driving-point immittance function; if the network is a two-terminal-pair network, then G(s) is a transfer function.

Whereas equation (38) represents the output of a single-capacitor CN, it does not readily provide the desired insight into the operational characteristics. To obtain more insight, the CN will be specified as the two-terminal-pair active CN, shown in Figure 16. The noncommutated transfer function, G(s), as shown in the equivalent circuit of Figure 17, is

$$G(s) = \frac{\alpha}{\tau s + 1} , \tag{39}$$

where α is $-\frac{R_1}{R_0}$ and τ is $R_1 C_1$.

Substituting equation (39) into equation (38), we see that

$$Y(s) = -\frac{4\alpha}{\pi^2} \sum_{r=-\infty}^{+\infty} X(s - j2\omega_0 r)\, \epsilon^{j2\phi r} \sum_{\substack{\ell=1 \\ \text{odd}}}^{\infty} \left\{ \frac{1}{\ell(2r-\ell)\left[(\tau s+1) - j\tau\ell\omega_0\right]} - \frac{1}{\ell(2r+\ell)\left[(\tau s+1) + j\tau\ell\omega_0\right]} \right\} . \tag{40}$$

Combining terms and using the identity of equation (B-5), or

$$\sum_{\substack{k=1 \\ \text{odd}}}^{\infty} \frac{1}{(k^2 - x^2)(k^2 + y^2)} = \frac{\frac{\pi}{4x} \tan \frac{\pi}{2} x - \frac{\pi}{4y} \tanh \frac{\pi}{2} y}{x^2 + y^2} , \tag{41}$$

we find that equation (40) can be simplified to

$$Y(s) = \frac{\alpha}{\pi} \sum_{r=-\infty}^{+\infty} \frac{X(s - j2r\omega_0)}{\left[(\tau s+1) - j2\tau r\omega_0\right]} \left\{ \frac{1}{r} \tan \pi r - \frac{2\tau\omega_0}{(\tau s+1)} \tanh \frac{\pi}{2} \left(\frac{\tau s+1}{\tau\omega_0} \right) \right\} \epsilon^{j2r\phi} . \tag{42}$$

Equation (42) can also be written as

$$Y(s) = X(s)\,\frac{\alpha}{\tau s+1}\left\{1 - \frac{2\tau\omega_0}{\pi(\tau s+1)}\tanh\frac{\pi}{2}\left(\frac{\tau s+1}{\tau\omega_0}\right)\right\}$$

$$- \frac{2\alpha\tau\omega_0}{\pi(\tau s+1)}\tanh\frac{\pi}{2}\left(\frac{\tau s+1}{\tau\omega_0}\right)\sum_{r=-\infty}^{+\infty}{}' \frac{X(s-j2r\omega_0)\,\epsilon^{j2r\phi}}{[(\tau s+1)-j2r\omega_0\tau]}\,, \tag{43}$$

where the symbol $\sum_{r=-\infty}^{+\infty}{}'$ indicates the summation over all values of r except r = 0. Examination of equation (43) shows that for a sinusoidal input signal, the output signal is composed of a signal component at the input signal frequency ω, and additional signal components at sideband frequencies of even multiples of the commutation frequency, i.e., at frequencies of $(\omega\pm2\omega_0)$, $(\omega\pm4\omega_0)$, etc. As a special case, when the input frequency equals the commutation frequency, $\omega = \omega_0$, the sideband signal frequencies are harmonics of the input signal frequency and are at frequencies $3\omega_0$, $5\omega_0$, $7\omega_0$, and so forth.

Frequency Response of the Single-Capacitor CN

For convenience, equation (43) can be rewritten as

$$Y(s) = F(o,s)\,X(s) + \sum_{r=-\infty}^{+\infty}{}' F(r,s)\,X(s-j2r\omega_0)\,\epsilon^{j2r\phi}, \tag{44}$$

where

$$F(o,s) = \frac{\alpha}{\tau s+1}\left\{1 - \frac{2\tau\omega_0}{\pi(\tau s+1)}\tanh\frac{\pi}{2}\left(\frac{\tau s+1}{\tau\omega_0}\right)\right\}, \tag{45}$$

and

$$F(r,s) = -\frac{2\alpha\tau\omega_0\tanh\frac{\pi}{2}\left(\frac{\tau s+1}{\tau\omega_0}\right)}{\pi(\tau s+1)(\tau s+1-j2r\tau\omega_0)}\,. \tag{46}$$

These equations are similar to those of Franks and Sandberg [11]. By applying bandlimiting restraints to the input and output signal frequencies, a transfer function can be defined as

$$\frac{Y(s)}{X(s)} = F(o,s), \tag{47}$$

where

$$\begin{aligned} \frac{Y(j\omega)}{X(j\omega)} &= F(o, j\omega) \quad \text{in } |\omega| < N\omega_0, \\ &= 0 \quad \text{in } |\omega| > N\omega_0, \end{aligned} \tag{48}$$

and where $N = 1$ for the single-capacitor case and ω_0 is the commutation frequency. The allowable frequency band in equation (48) is double the frequency band specified by Franks and Sandberg because of the half-period phasing of the commutation functions.

We will now investigate the frequency response of the single-capacitor CN beyond the frequency range imposed by the restraint given in equation (48). Writing out the first few terms of the infinite series in equation (44), we find that

$$\begin{aligned} Y(s) &= F(o,s)\,X(s) + F(1,s)\,X(s-j2\omega_0)\,\epsilon^{j2\phi} \\ &+ F(-1,s)\,X(s+j2\omega_0)\,\epsilon^{-j2\phi} + F(2,s)\,X(s-j4\omega_0)\,\epsilon^{j4\phi} \\ &+ F(-2,s)\,X(s+j4\omega_0)\,\epsilon^{-j4\phi} + \ldots \quad . \end{aligned} \tag{49}$$

Dividing both sides of equation (49) by $X(s)$, we see that

$$\begin{aligned} \frac{Y(s)}{X(s)} &= F(o,s) + F(1,s)\,\frac{X(s-j2\omega_0)}{X(s)}\,\epsilon^{j2\phi} + F(-1,s)\,\frac{X(s+j2\omega_0)}{X(s)}\,\epsilon^{-j2\phi} \\ &+ F(2,s)\,\frac{X(s-j4\omega_0)}{X(s)}\,\epsilon^{j4\phi} + F(-2,s)\,\frac{X(s+j4\omega_0)}{X(s)}\,\epsilon^{-j4\phi} + \ldots \quad . \end{aligned} \tag{50}$$

The Laplace transform for an input sinusoidal signal with a maximum amplitude of one ($x(t) = 1 \sin \omega t$) is

$$X(s) = \frac{\omega}{s^2 + \omega^2} \tag{51}$$

and therefore

$$X(s - j2r\omega_0) = \frac{\omega}{(s - j2r\omega_0)^2 + \omega^2} \tag{52}$$

where ω is the frequency of the input signal and $r = \pm 1, \pm 2, \pm 3, \ldots$. Substituting equations (51) and (52) into the right side of equation (50), we see that

$$\left[\frac{Y(s)}{X(s)}\right]^* = F(o,s) + F(1,s)\,\frac{(s^2+\omega^2)\,\epsilon^{j2\phi}}{(s - j2\omega_0)^2+\omega^2} + F(-1,s)\frac{(s^2+\omega^2)\,\epsilon^{-j2\phi}}{(s+j2\omega_0)^2+\omega^2}$$

$$+ F(2,s)\,\frac{(s^2+\omega^2)\,\epsilon^{j4\phi}}{(s - j4\omega_0)^2+\omega^2} + F(-2,s)\,\frac{(s^2+\omega^2)\,\epsilon^{-j4\phi}}{(s+j4\omega_0)^2+\omega^2} + \ldots \tag{53}$$

where $\left[\frac{Y(s)}{X(s)}\right]^*$ denotes that the input is a sinusoidal signal described by equation (51). When the input signal frequency ω is equal to ω_0, equation (53) becomes

$$\left[\frac{Y(s)}{X(s)}\right]^* = F(o,s) + F(1,s)\,\frac{(s+j\omega_0)\,\epsilon^{j2\phi}}{(s - j3\omega_0)} + F(-1,s)\,\frac{(s - j\omega_0)\,\epsilon^{-j2\phi}}{(s+j3\omega_0)}$$

$$+ F(2,s)\frac{(s+j\omega_0)\,(s - j\omega_0)\,\epsilon^{j4\phi}}{(s - j3\omega_0)\,(s - j5\omega_0)}$$

$$+ F(-2,s)\,\frac{(s+j\omega_0)\,(s - j\omega_0)\epsilon^{-j4\phi}}{(s+j3\omega_0)\,(s+5j\omega_0)} + \ldots \tag{54}$$

To compute the frequency response $\frac{Y(j\omega)}{X(j\omega)}$, s is replaced by $j\omega$ in equation (53). For all frequencies ω, except integral values of the commutation frequency ω_0,

the first term in equation (53) yields the value of the frequency response, that is, $F(o, j\omega)$. The second term and all subsequent terms are identically zero. Although the frequency response is concerned only with the component in the output signal at the same frequency as the input signal, it should be remembered that the output signal of a CN is composed of an infinite number of signal components at different frequencies.

When the input signal frequency is equal to ω_0, the value of the frequency response will be given by equation (54) and will consist of just the first two terms, or

$$\frac{Y(j\omega_0)}{X(j\omega_0)} = F(o, j\omega_0) + F(1, j\omega_0)(-1)\epsilon^{j2\phi}. \tag{55}$$

For the frequency response at other integral values of the commutation frequency ω_0, ω in equation (53) is replaced by $n\omega_0$, where $n \pm 2, 3, 4, \ldots$, and the value is computed as was done for ω_0 in equation (55). The single-capacitor CN with an input signal frequency equal to the commutation frequency is characterized, at the commutation frequency, by equation (55). The phase parameter ϕ in equation (55) will obviously affect the value of the frequency response. The extent of this effect will now be determined for two values of ϕ, $\phi = 0$, and $\phi = \pi/2$.

For the case where $\phi = 0$, equation (55) becomes

$$\frac{Y(j\omega_0)}{X(j\omega_0)} = F(o, j\omega_0) - F(1, j\omega_0) . \tag{56}$$

The values of $F(o, j\omega_0)$ and $F(1, j\omega_0)$ from equations (45) and (46), respectively, assuming a value of $\tau\omega_0 = 2\pi$, are

$$F(o, j\omega) = (0.407 - j0.026)\alpha \tag{57}$$

and

$$F(1, j\omega_0) = -(0.404)\alpha . \tag{58}$$

Substituting the values of $F(o, j\omega_0)$ and $F(1, j\omega_0)$ into equation (56), we find that

$$\frac{Y(j\omega_0)}{X(j\omega_0)} = (0.811 - j0.026)\propto . \tag{59}$$

To have the amplitude of the frequency response equal to unity at the commutation frequency, $\propto$ should be $1.234 \left(\frac{\pi^2}{8}\right)$. If the input signal frequency were some value other than ω_0, either slightly smaller or larger (that is, $\omega = \omega_0 - \epsilon$ or $\omega = \omega_0 + \epsilon$, where ϵ is some small positive number), then all the terms, except the first, on the right side of equation (53) would vanish. The frequency response would then be equal to $F(o, j\omega)$ and it would have the approximate value given by equation (57). For an $\propto$ of $\frac{\pi^2}{8}$, the amplitude of $F(o, j\omega)$ would be approximately equal to one-half; therefore, the amplitude of the frequency response of the single-phase CN jumps to approximately twice its former value when ω equals ω_0.

For the case where $\phi = \pi/2$, again letting $\tau\omega_0 = 2\pi$ and $\propto = \frac{\pi^2}{8}$, we see that equation (55) becomes

$$\frac{Y(j\omega_0)}{X(j\omega_0)} = F(o, j\omega_0) + F(1, j\omega_0) \tag{60}$$

or

$$\frac{Y(j\omega_0)}{X(j\omega_0)} = \propto (0.003 - j0.026) = 0.032 \angle -83^\circ . \tag{61}$$

The foregoing analysis has shown the frequency response for a single-capacitor CN to be phase sensitive at the commutation frequency. For a change in the phase parameter from $\phi = 0$ to $\phi = \pi/2$ radians, the frequency response amplitude was reduced by 96 percent. Using $\tau\omega_0 = 2\pi$ and $\propto = \frac{\pi^2}{8}$, we calculated the reduction in the frequency response amplitude for ω equal to $2\omega_0$ and $3\omega_0$ for the same variation in the phase parameter ϕ and the same transfer function. The results together with experimental results for the same transfer function and set of parameters are as follows.

Frequency - ω	Calculated Value (Percent reduction)	Experimental Value (Percent reduction)
ω_0	96.8	95
$2\omega_0$	2.5	Negligible
$3\omega_0$	53.5	54.5

Inspection of equation (53) reveals that the jump phenomena just examined at ω_0 occur at all integral values of the commutation frequency. Therefore, the frequency response amplitude characteristic of the single-capacitor CN is a quasi-continuous function with jump phenomena occurring at frequencies of $n\omega_0$, where n is 1, 2, 3, ... The value of the network's amplitude frequency response at the point of discontinuity, $n\omega_0$, is a function of the phase parameter ϕ. It can also be deduced from equation (53) that the quasi-continuous property of the amplitude frequency response is an inherent property of the CN resulting from the frequency translated components in the output signal and does not depend on any particular network structure.

To verify the preceding analytical results, an experiment was run on a single-capacitor CN with the same parameter values that were used in the foregoing analysis. The results are shown in the amplitude frequency response plot of Figure 24. As previously shown, there was good agreement between analytical and experimental results. Appendix A gives the details of the experimental procedures used for this work.

Single-Phase Multicapacitor CN's

In Figure 15 the block titled "Analysis of Multicapacitor CN" has four sub-blocks, one of which is a single-phase CN. Almost all multicapacitor CN's employing single-phase commutation (that is, all the commutation functions are exactly in phase with each other) can be reduced easily to the CN equivalent block diagram by applying Lemma I.1 and Theorem I. The resulting system function, G(s), can then be substituted into equation (38) to determine the system's frequency response characteristics and subsequently its transient and steady-state operating characteristics. Finding the inverse of the output, Y(s), in equation (38) will usually be very difficult and only an approximation will be given for most cases.

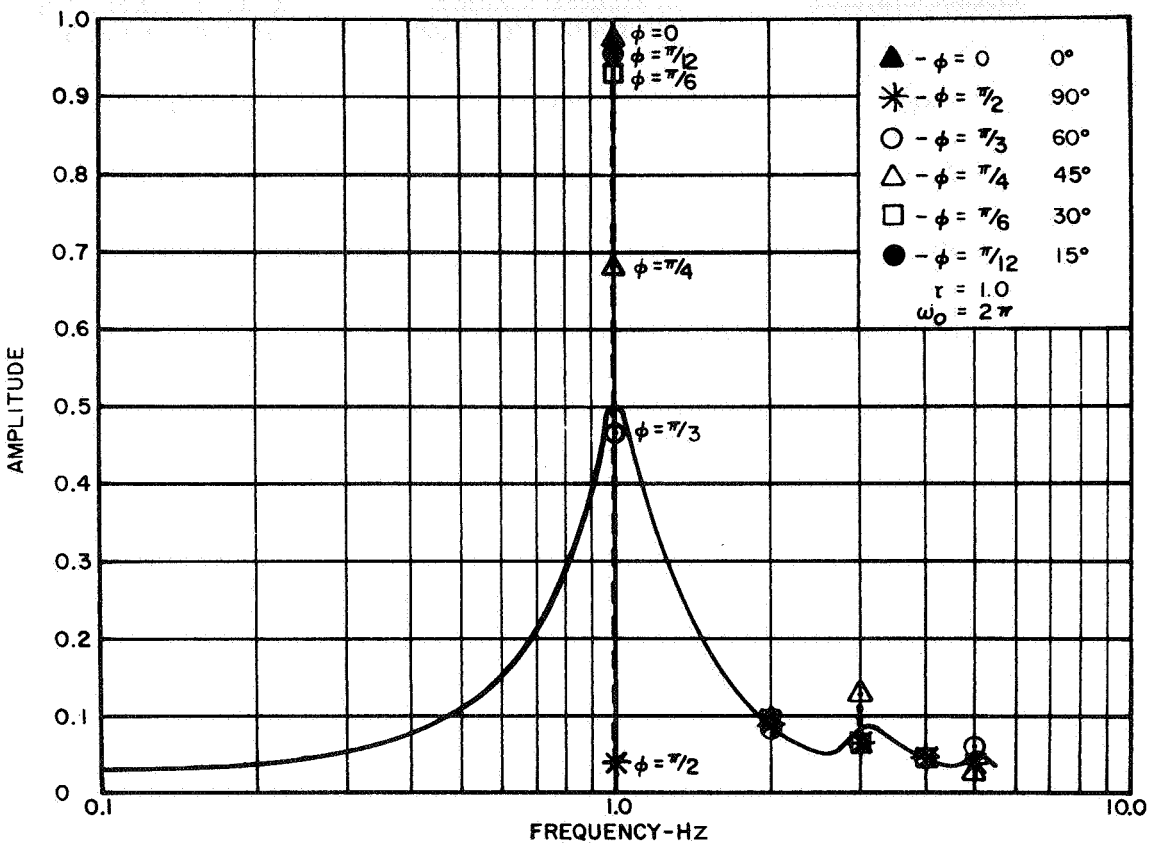

FIGURE 24. EXPERIMENTAL AMPLITUDE FREQUENCY RESPONSE FOR SINGLE-CAPACITOR CN (τ = 1.0 SECOND)

Single-phase multicapacitor CN's have many of the same characteristics as the single-capacitor CN. If two or more single-phase CN's are connected in cascade as shown in Figure 25(a), they can be reduced to the equivalent circuit of Figure 25(b) since $p_1(t)$ is equal to $p_2(t)$ and $p_1(t) \cdot p_2(t) = 1$. The same procedure would apply for any other units connected in cascade with no intervening frequency dependent elements.

If two or more single-phase CN's are connected in parallel as shown in Figure 26(a), they can be represented as shown in Figure 26(b). Additional units in parallel would be treated in the same way. These two examples demonstrate the relatively simple manipulations required for handling multicapacitor single-phase CN's.

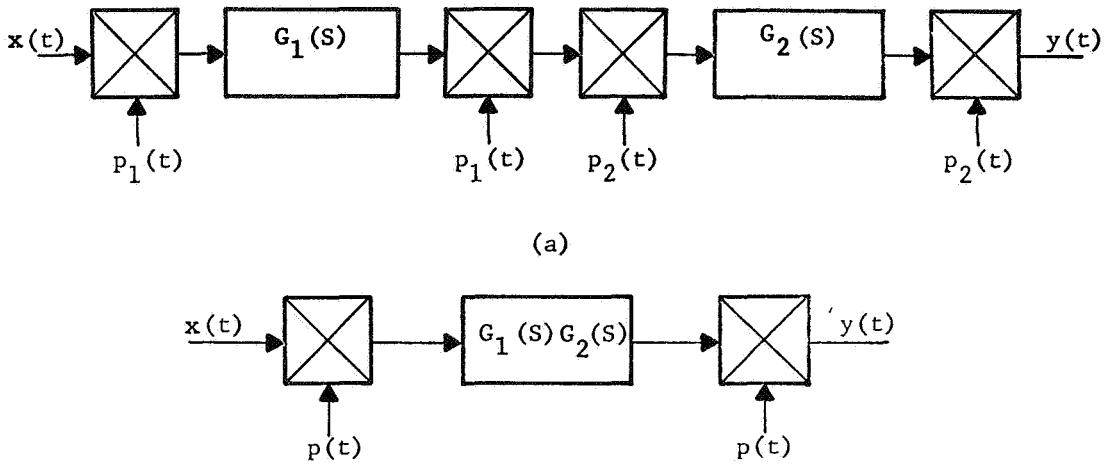

FIGURE 25. CASCADED SINGLE-PHASE CN'S

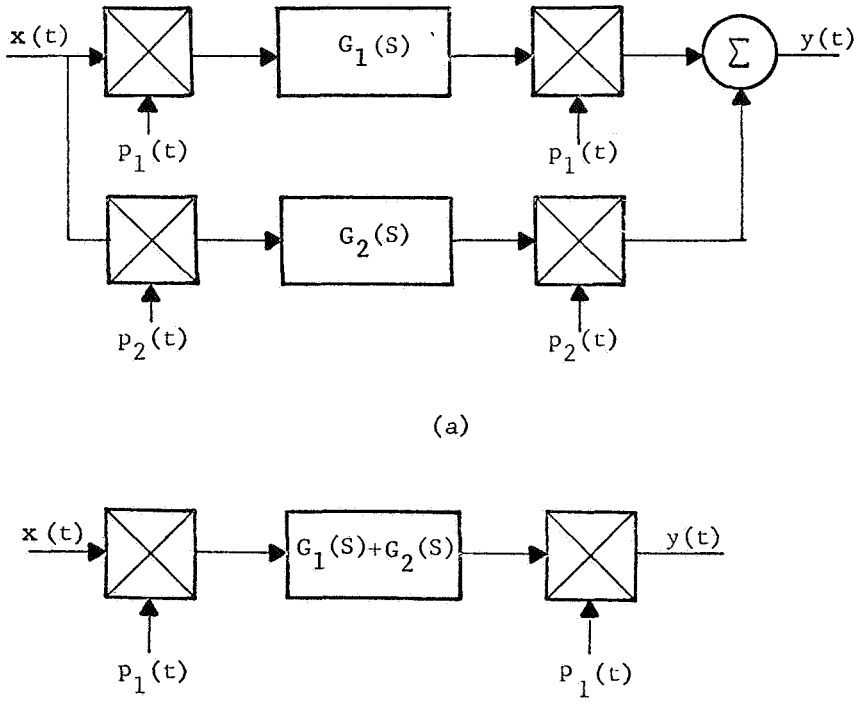

FIGURE 26. PARALLELED CONNECTION OF SINGLE-PHASE CN'S

Commutated Network Parameters

There are three basic parameters governing the operating characteristics of the CN's considered in this section. Two of these parameters are associated with the noncommutated system function G(s) and the other parameter is associated with the commutation function. The commutation functions are assumed perfect square waves of unity amplitude; hence their only parameter is frequency ω_0. The system functions considered in this section are simple lag networks composed of resistors and capacitors, so there are at most two factors: a gain α and a time constant τ, or break-frequency $\omega_c = \frac{1}{\tau}$.

The commutation of the reactive or energy storing elements of a CN has the basic effect of transforming the frequency response characteristics, either low-pass or high-pass, into a band-pass or into band-elimination characteristics, respectively. The center frequency of the band-pass or band-elimination characteristics will be approximately equal to the commutation frequency ω_0. The bandwidth of the CN is a function of the network's time constant τ. The definition of bandwidth for a CN will be the same as for a noncommutated network. For a single-capacitor, simple-lag CN, as shown in Figure 16, a variation in the time-constant results in a family of frequency response curves as shown in Figures 27 and 28. (The jump phenomena of the amplitude response were not included in Figure 27.) The curves in Figure 27 show that as τ increases, the bandwidth decreases and when τ decreases, the bandwidth increases. These results coincide with the frequency response characteristics of the noncommutated transfer function $\frac{\alpha}{\tau s + 1}$ to variations in the parameter τ.

From Figure 27 it is obvious that a limitation exists on the transformation of the low-pass noncommutated network characteristics to the band-pass CN characteristics. This limitation was found to be a function of the dominating parameters of the CN; that is, the time constant τ of the noncommutated system function and the commutation frequency ω_0. The frequency response curves of Figures 27 and 28 were obtained by plotting the first term of equation (43) as a function of ω, or

$$\frac{Y(j\omega)}{X(j\omega)} = \frac{\alpha}{1+j\tau\omega} \left\{ 1 - \frac{2\tau\omega_0}{\pi(1+j\tau\omega)} \tanh \frac{\pi}{2} \left(\frac{1+j\tau\omega}{\tau\omega_0} \right) \right\}, \qquad (62)$$

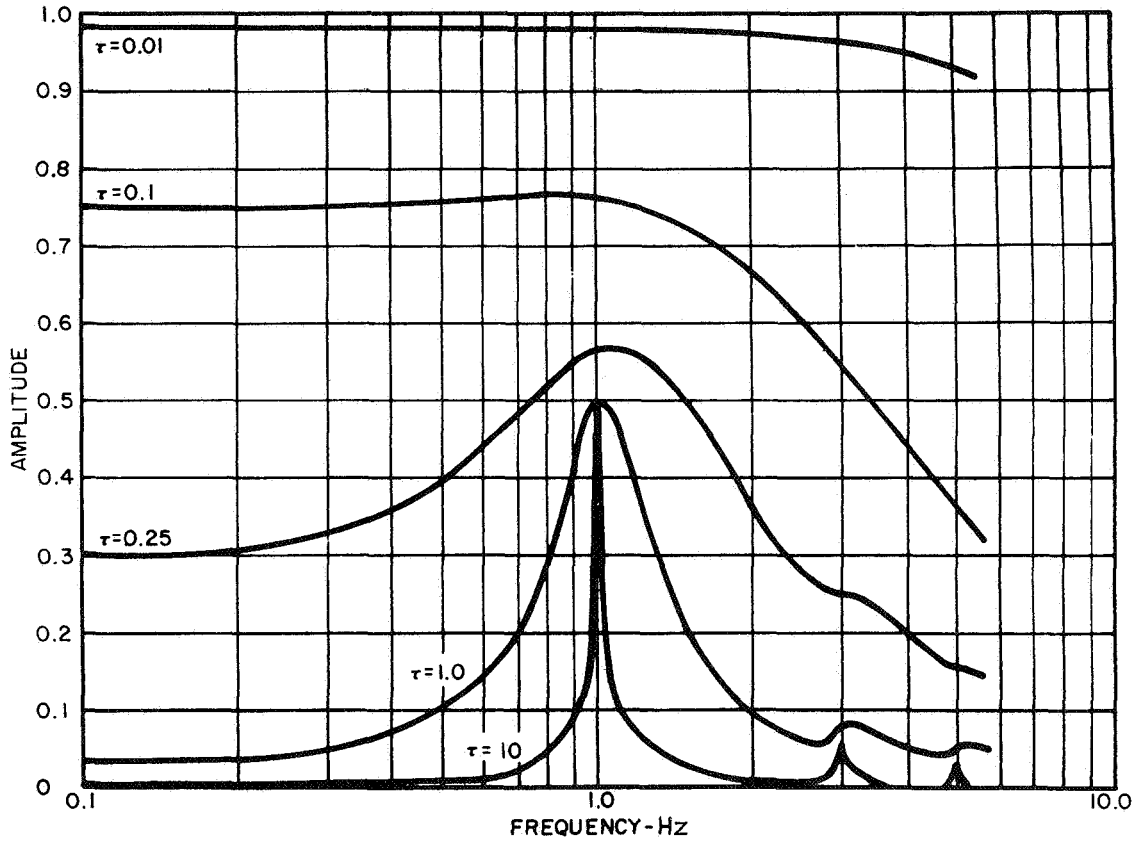

FIGURE 27. AMPLITUDE FREQUENCY RESPONSE OF A SINGLE-CAPACITOR CN

where s has been replaced by $j\omega$. For equation (62) to yield an ideal band-pass characteristic, the value of equation (62) should be essentially zero for small values of ω. This can be expressed as

$$\left(1 - \frac{2\tau\omega_0}{\pi} \tanh \frac{\pi}{2\tau\omega_0}\right) \approx 0 . \tag{63}$$

The above approximation will hold for values of $\tau\omega_0 \geqq 2\pi$. Since $\omega_c = \frac{1}{\tau}$, a good band-pass characteristic will be obtained if the ratio of the commutation frequency to the lag network break-frequency is approximately equal to six, or

$$\frac{\omega_0}{\omega_c} \approx 6. \tag{64}$$

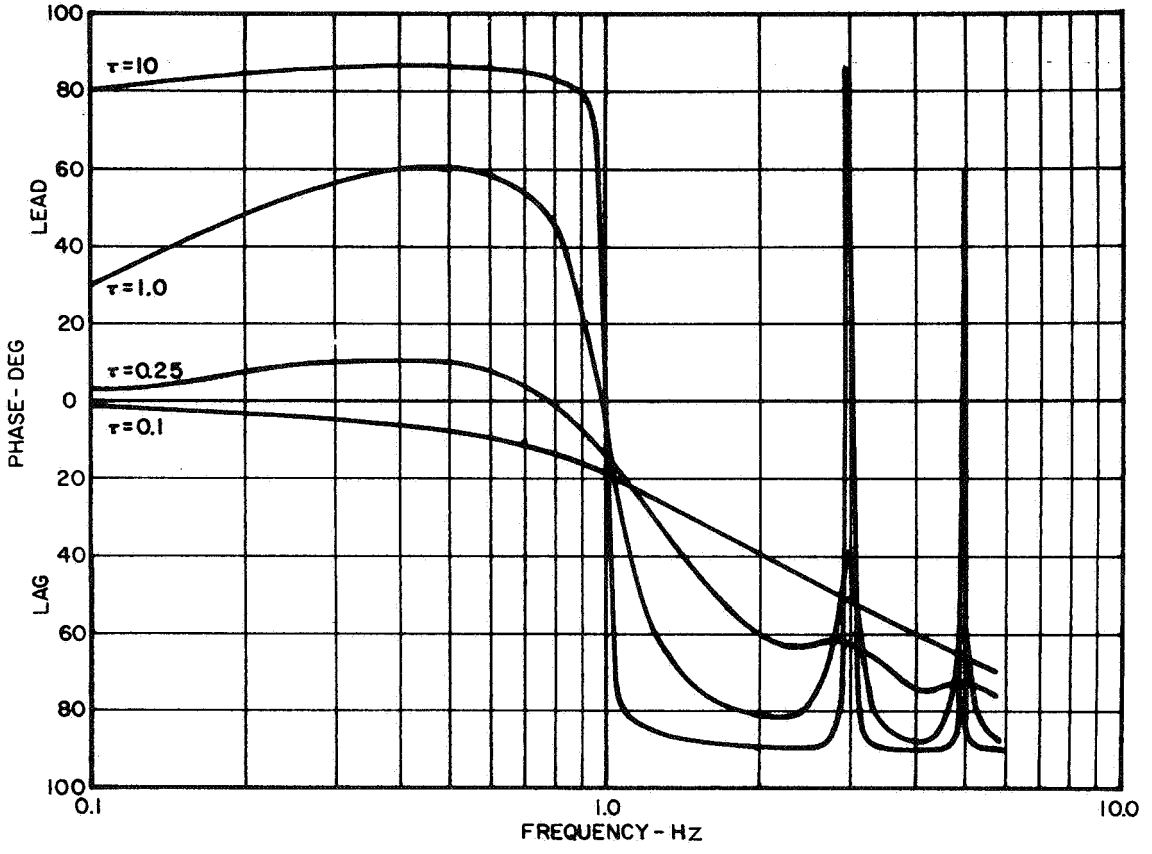

FIGURE 28. PHASE FREQUENCY RESPONSE OF A SINGLE-CAPACITOR CN

The gain factor α of G(s) determines the gain of the overall network. The value of α can be extremely important in some cases, such as using CN's with band-pass characteristics to form notch filters. For the notch filter case, the number of parallel paths in the equivalent circuit determines the value of α necessary to have unity gain at the commutation frequency ω_0 [15].

POLYPHASE COMMUTATED NETWORKS

General

A polyphase CN employs two or more commutation functions to commutate a corresponding number of capacitors. In this investigation the commutation functions are uniformly delayed by T/2N seconds, where T is the period

of commutation and N is the number of phases. For a two-phase CN (N=2), the time delay between the two commutation functions would be T/4 seconds, or $\frac{\pi}{2\omega_0}$ seconds, since $T = \frac{2\pi}{\omega_0}$ seconds.

Polyphase CN's are usually employed to solve two problems that occur when single-phase CN's are used and the problems are:

1. Phase sensitivity, that is, the dependency of the output on the phase of the input signal with respect to the commutation function, which is inherent to the single-capacitor CN at integral values of the commutation frequency.

2. The harmonics or sideband signals in the CN output signal.

For the CN's considered in this section, all of the commutation functions have the same operating frequency, ω_0. Hart [2] discusses an application of polyphase CN's in which more than one commutation frequency is used.

Analysis of Polyphase CN's

The effectiveness of the polyphase CN to resolve the two problems mentioned above depends on the number of capacitors used and the phasing of the associated commutating functions. Early experimental work showed that a two-capacitor CN, with the second commutation function having a T/4 second time delay with respect to the first commutation function, was phase insensitive in the frequency range $0 \leq \omega < 2\omega_0$ even at the frequency $\omega = \omega_0$. It will now be shown why the two-capacitor CN, illustrated in Figure 29, is phase insensitive at the commutation frequency ω_0. Designating $p_1(t)$ as the analytical expression for the switching function $s(\omega_0 t)$ and $p_2(t)$ for $s(\omega_0 t - \frac{\pi}{2})$, and assuming $C_1 = C_2$, $R_0 = R_2$, and $R_1 = R_3$, we see that the total output of the CN in the s domain can be written as

$$Y(s) = Y_1(s) + Y_2(s) \tag{65}$$

where $Y_1(s)$ and $Y_2(s)$ are the Laplace transforms of $y_1(t)$ and $y_2(t)$, respectively. Using the procedures shown in the preceding section, we see that the outputs $Y_1(s)$ and $Y_2(s)$ can be expressed in the form of equation (44), or

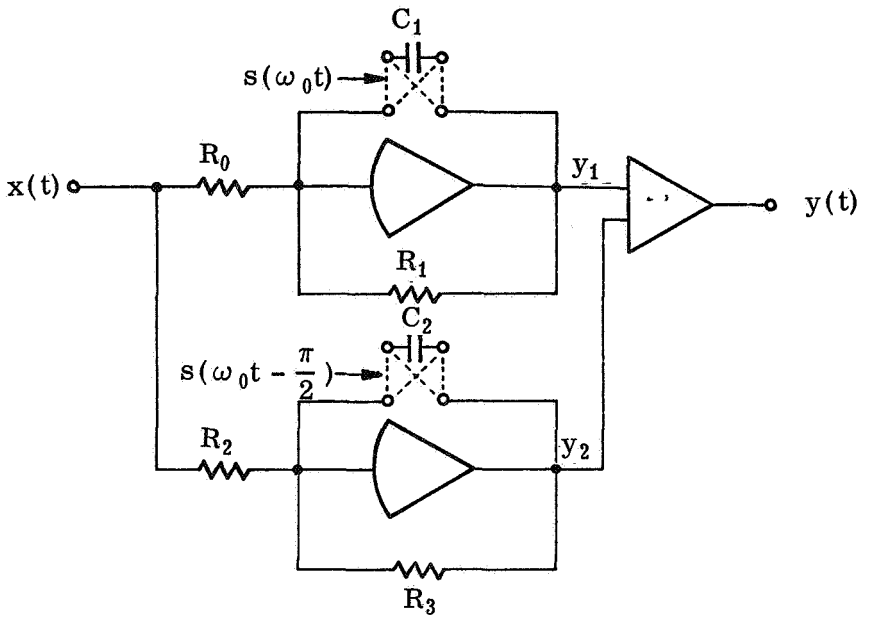

FIGURE 29. TWO-CAPACITOR CN

$$Y_1(s) = F_1(o,s)\ X(s) + \sum_{r=-\infty}^{+\infty}{}' F_1(r,s)X(s-j2r\omega_0)\ \epsilon^{j2r\phi} \tag{66}$$

and

$$Y_2(s) = F_2(o,s)\ X(s) + \sum_{r=-\infty}^{+\infty}{}' F_2(r,s)X(s-j2r\omega_0)\ \epsilon^{j2r(\phi-\frac{\pi}{2})}. \tag{67}$$

Because the elements of the two networks have the same values, $F_1(o,s) = F_2(o,s)$ and $F_1(r,s) = F_2(r,s)$. The frequency responses of the two CN's at the commutation frequency, obtained by using equation (55), can be written as

$$\frac{Y_1(j\omega_0)}{X(j\omega_0)} = F(o,j\omega_0) + F(1,\ j\omega_0)\ (-1)\epsilon^{j2\phi} \tag{68}$$

and

$$\frac{Y_2(j\omega_0)}{X(j\omega_0)} = F(o,\ j\omega_0) + F(1,\ j\omega_0)(-1)\epsilon^{j2(\phi - \frac{\pi}{2})} \quad . \tag{69}$$

By adding equations (68) and (69) to obtain the total frequency response

$$\begin{aligned}\frac{Y(j\omega_0)}{X(j\omega_0)} &= F(o, j\omega_0) - F(1, j\omega_0)\epsilon^{j2\phi} \\ &+ F(o, j\omega_0) - F(1, \omega_0)\epsilon^{j2(\phi - \frac{\pi}{2})} \\ &= 2\,F(o, j\omega_0)\end{aligned} \tag{70}$$

because $\epsilon^{j2(\phi - \pi/2)}$ is $-\epsilon^{j2\phi}$. Thus, the phase parameter ϕ has been eliminated from the frequency response described by equation (70). The CN is, therefore, insensitive to the phase relationship between the input signal and the commutation functions at the frequency ω_0. It is apparent, from equation (70), that the time delay of T/4 seconds between the commutation function $p_1(t)$ and $p_2(t)$ is necessary to eliminate the phase parameter ϕ. These results lead to the following theorem.

Theorem II

> If an uncoupled CN consisting of resistors and capacitors is excited by a sinusoidal signal and the capacitors are being perfectly commutated at a frequency ω_0, then to transmit all the information contained in the input signal for the frequency range $0 \leq \omega < N\omega_0$, assuming a random phase relationship exists between the commutating functions and the input signal when the input signal's frequency equals ω_0, there must be at least N-forward paths in the equivalent block diagram of the commutated network and the commutation functions for the N-paths must have a $\frac{\pi}{N\omega_0}$-second time delay relationship between each other, or the statements

$$
\begin{aligned}
p_1(t) &= s(\omega_0 t) \\
p_2(t) &= s(\omega_0[t - \frac{\pi}{N\omega_0}]) \\
p_3(t) &= s(\omega_0[t - \frac{2\pi}{N\omega_0}]) \\
&\vdots \\
p_i(t) &= s(\omega_0[t - \frac{(i-1)\pi}{N\omega_0}]) \\
&\vdots
\end{aligned}
\tag{71}
$$

must hold true where the $p_i(t)$'s are the commutating functions and

$i = 1, 2, 3, \ldots N.$

Up to this point, the CN's with multicapacitors have been composed of "uncoupled" single-capacitor CN's. The distinction between "uncoupled" and "coupled" CN's is illustrated in Figure 30(a) and (b), respectively. Whereas the difference between the coupled and uncoupled circuits of Figure 30 is not readily apparent, the associated equivalent block diagrams of Figure 31 clearly show the major difference. The difference is that in the uncoupled case, the input to each commutated circuit is simply the input signal $x(t)$. However, in the coupled case, the input signal into each commutated circuit contains the input signal $x(t)$ plus the total output signal $y(t)$ modified by a gain factor K. The total output signal $y(t)$ contains all the sideband frequencies or harmonics of each commutated circuit in addition to a component at the input signal frequency.

Proof of Theorem II. The proof of Theorem II is based on the results of the one-capacitor CN analysis. The expression for the output of the single-capacitor simple-lag network of Figure 16 is given by equation (42) where

$$
Y(s) = \frac{\alpha}{\pi} \sum_{r=-\infty}^{+\infty} \frac{X(s - j2r\omega_0)\, \epsilon^{j2r\phi}}{[(\tau s + 1) - j2r\tau\omega_0]} \left\{ \frac{1}{r} \tan r\pi - \frac{2\tau\omega_0}{(\tau s + 1)} \tanh \frac{\pi}{2} \left(\frac{\tau s + 1}{\tau\omega_0} \right) \right\}. \tag{42}
$$

It was shown that for $s = j\omega_0$, the value of the frequency response $\frac{Y(j\omega_0)}{X(j\omega_0)}$ varies from one to approximately zero depending upon the phase parameter ϕ (assuming the gain factor $\alpha = -\frac{\pi^2}{8}$ and $\tau\omega_0 = 2\pi$). If an uncoupled CN is assumed to have N-capacitors, and the corresponding commutating functions have a time delay of $\frac{\pi}{N\omega_0}$ seconds with respect to each other, then from the i^{th} path of the equivalent block diagram the output is

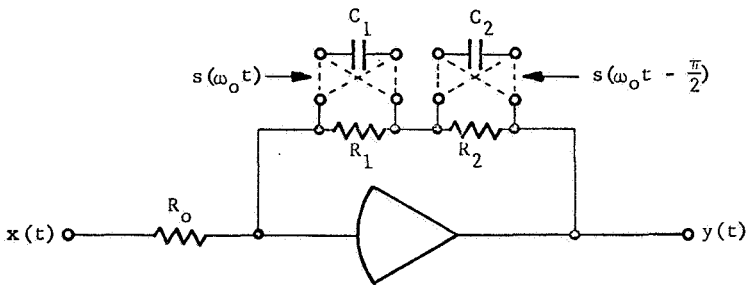

(a) UNCOUPLED

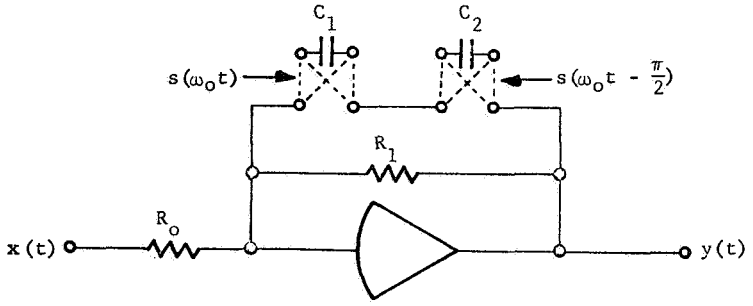

(b) COUPLED

FIGURE 30. COMMUTATED NETWORKS

$$Y_i(s) = \frac{\alpha}{\pi} \sum_{r=-\infty}^{+\infty} \frac{X(s - j2r\omega_0)}{[(\tau s + 1) - j2r\omega\tau]} \epsilon^{j2r(\phi - \frac{i-1}{N}\pi)} \left\{ \frac{1}{r} \tan \pi r - \frac{2\tau\omega_0}{(\tau s + 1)} \tanh \frac{\pi}{2} \left(\frac{\tau s + 1}{\tau \omega_0} \right) \right\} \tag{72}$$

where $i = 1, 2, \ldots, N$.

The equivalent block diagram for an N-capacitor CN is shown in Figure 32. According to Theorem II, this circuit will be insensitive to the phase parameter ϕ for $\omega < N\omega_0$. This will be shown to be true in the following manner: by using the same notation as that in the preceding section, after dividing both sides of equation (72) by X(s), the frequency response of the i^{th} path can be expressed as

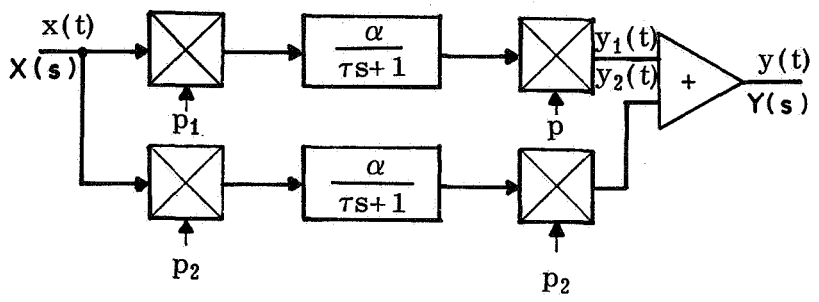

(a) UNCOUPLED

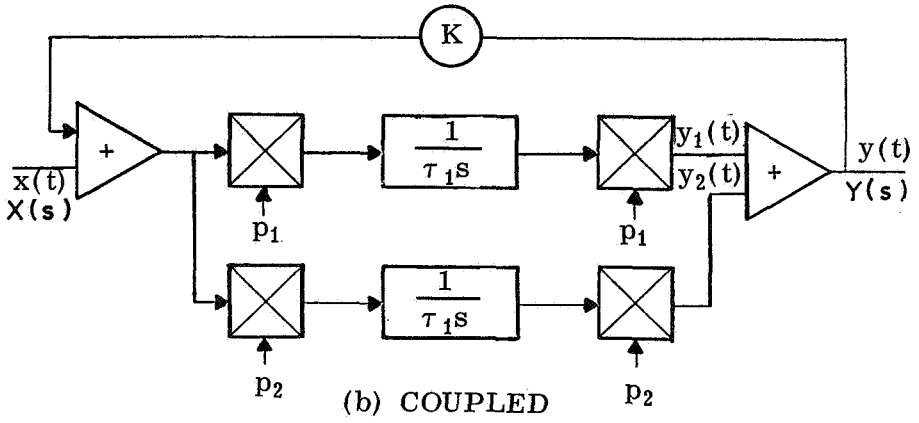

(b) COUPLED

FIGURE 31. CN EQUIVALENT BLOCK DIAGRAMS

$$\frac{Y_i(j\omega)}{X(j\omega)} = \sum_{r=-\infty}^{+\infty} F(r, j\omega)\, \frac{X(j\omega - j2r\omega_0)}{X(j\omega)}\, \epsilon^{j2r\left(\phi - \frac{i-1}{N}\pi\right)}. \qquad (73)$$

Based on the frequency response analysis already given, the value of equation (73) at any frequency other than integral values of ω_0 is just $F(o, j\omega)$. For any lower positive integral multiple of ω_0 less than $N\omega_0$, equation (73) can be expressed as

$$\frac{Y_i(j\ell\omega_0)}{X(j\ell\omega_0)} = \sum_{r=-\infty}^{+\infty} F(r, j\ell\omega_0)\, \frac{X(j\ell\omega_0 - j2r\omega_0)}{X(j\ell\omega_0)}\, \epsilon^{j2r\left(\phi - \frac{i-1}{N}\pi\right)} \qquad (74)$$

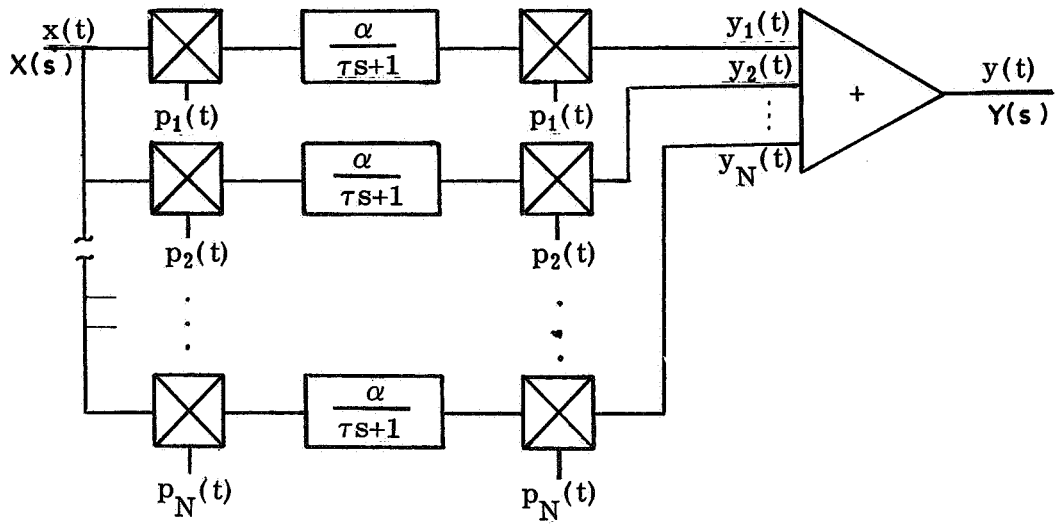

FIGURE 32. N-PATH UNCOUPLED CN

where ℓ is a positive integer and $\ell < N$. For a sinusoidal input signal, equation (74) can be shown to reduce to

$$\frac{Y_i(j\ell\omega_0)}{X(j\ell\omega_0)} = F(o, j\ell\omega_0) + F(\ell, j\ell\omega_0)(-1)\,\epsilon^{j2\ell(\phi - \frac{i-1}{N}\pi)}. \tag{75}$$

The value of the total frequency response of Figure 32 at $\omega = \ell\,\omega_0$ can be written as

$$\frac{Y(j\ell\omega_0)}{X(j\ell\omega_0)} = \sum_{i=1}^{N} \frac{Y_i(j\ell\omega_0)}{X(j\ell\omega_0)}. \tag{76}$$

By substituting equation (75) into equation (76) and performing the indicated summation

$$\frac{Y(j\ell\omega_0)}{X(j\ell\omega_0)} = N\,F(o, j\ell\omega_0) - F(\ell, j\ell\omega_0)\epsilon^{j2\ell\phi}\left\{\epsilon^{-jo} + \epsilon^{-j2\pi\ell\frac{1}{N}} + \epsilon^{-j2\pi\ell\frac{2}{N}} + \ldots + \epsilon^{-j2\pi\ell\frac{N-1}{N}}\right\}. \tag{77}$$

The expression enclosed in the braces is a finite geometric series with a value of zero for all $\ell < N$ and a value of N for $\ell = N$. For $\ell < N$ the frequency response for the CN of Figure 32 is given by the first term only of equation (77). For $\ell = N$ the frequency response at $\omega = N\omega_0$ is given by

$$\frac{Y(jN\omega_0)}{X(jN\omega_0)} = N\,F(o, jN\omega_0) - N\,F(N, jN\omega_0)\,\epsilon^{j2N\phi} \tag{78}$$

The frequency response of the CN of Figure 32 is therefore phase sensitive at the frequency $N\omega_0$, or it is a discontinuous function at that frequency. Below the frequency $N\omega_0$, the frequency response is a continuous function and is insensitive to the phase parameter ϕ, as shown by equation (77). This completes the proof of Theorem II.

It will now be shown that the circuits of Figures 29 and 30(a) are equivalent if the resistors of Figure 29 are properly selected. The total output for the CN of Figure 29 can be expressed as

$$y(t) = y_1(t) + y_2(t). \tag{79}$$

It can be shown [1] that for Figure 29

$$\frac{d(p_1y_1)}{dt} + \frac{p_1}{\tau_1}\,y_1 = \frac{\alpha_1}{\tau_1}\,p_1\,x \tag{80}$$

and

$$\frac{d(p_2y_2)}{dt} + \frac{p_2}{\tau_2}\,y_2 = \frac{\alpha_2}{\tau_2}\,p_2\,x \tag{81}$$

where

$$p_1 = p_1(t) = s(\omega_0 t),\ p_2 = p_2(t) = s(\omega_0 t - \frac{\pi}{2}),\ \tau_1 = R_1C_1,$$

$$\tau_2 = R_3C_2,\ \alpha_1 = -\frac{R_1}{R_0},\ \text{and}\ \alpha_2 = -\frac{R_3}{R_2}.$$

For $R_1 = R_3$, $R_0 = R_2$, and $C_1 = C_2$, then $\alpha_1 = \alpha_2$ and $\tau_1 = \tau_2$.

The total output for the CN of Figure 30(a) is

$$y(t) = e_1(t) + e_2(t) \tag{82}$$

where $e_1(t)$ is the voltage across resistor R_1 and $e_2(t)$ is the voltage across resistor R_2. It can be shown [1] that

$$\frac{d(p_1 e_1)}{dt} + \frac{p_1}{\tau_3} e_1 = \frac{\alpha_3}{\tau_3} p_1 x \tag{83}$$

and

$$\frac{d(p_2 e_2)}{dt} + \frac{p_2}{\tau_4} e_2 = \frac{\alpha_4}{\tau_4} p_2 x \tag{84}$$

where $p_1 = s(\omega_0 t)$, $p_2 = s(\omega_0 t - \pi/2)$, $\tau_3 = R_1 C_1$, $\tau_4 = R_2, C_2$,

$\alpha_3 = -\frac{R_1}{R_0}$, $\alpha_4 = -\frac{R_2}{R_0}$, $R_1 = R_2$, and $C_1 = C_2$.

If R_1, R_3, R_0, C_1, and C_2 of Figure 29 are equal to R_1, R_2, R_0, C_1, and C_2 of Figure 30(a), respectively, then $\tau_1 = \tau_2 = \tau_3 = \tau_4$ and $\alpha_1 = \alpha_2 = \alpha_3 = \alpha_4$. The commutation functions for Figures 29 and 30(a) are the same; therefore, for the same input $x(t)$, the solution to equation (80) is the same as the solution to equation (83) and the solution of equation (81) is the same as the solution of equation (84). Consequently, $y_1(t) = e_1(t)$ and $y_2(t) = e_2(t)$ and the CN of Figure 29 is equivalent to Figure 30(a). Henceforth, the uncoupled CN that will be used for discussion will be of the form shown in Figure 30(a), while the coupled CN will be of the form shown in Figure 30(b).

Harmonics in a Commutated Network

The harmonics or sideband frequencies present in the output signal of a single-capacitor CN are described by equation (38) and result from switching the polarity of the capacitor with respect to the network's output terminals. For a sinusoidal input signal, the frequency spectrum of the single-capacitor output is shown in Figure 33. The amplitudes of the sideband frequencies shown are not to scale. As shown, the harmonic or sideband signals originate at even harmonics of the commutating frequency, when the input signal frequency is zero, $\omega = 0$. As the frequency, ω, of the input signal increases, the sideband signals shift toward the odd multiples of the commutating frequency, ω_0. When the input signal frequency equals the commutating signal frequency, $\omega = \omega_0$, the output harmonics are all odd harmonics of ω_0. As the input signal frequency becomes greater than ω_0, the sideband signal frequencies continue to shift in the directions shown in Figure 33. Thus, at an input signal frequency of $2\omega_0$, there will be a component in the output at $\omega = 0$, $2\omega_0$, $4\omega_0$, $6\omega_0$, and so forth.

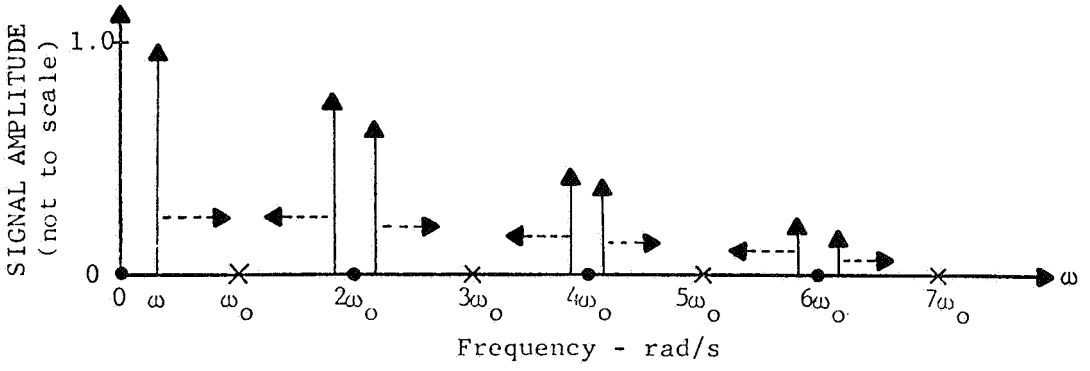

FIGURE 33. FREQUENCY SPECTRUM FOR SINGLE-CAPACITOR CN OUTPUT

The harmonics present in the output of an uncoupled polyphase CN are a direct function of the number of commutation functions and their relative phasing. The validity of this statement is not apparent from the basic equation for the single-capacitor CN, equation (38). By including a phasing term for the commutation functions and summing over the N-paths, the output for the polyphase CN of Figure 32 can be written as

$$Y(s) = \frac{\alpha}{\pi} \sum_{i=1}^{N} \sum_{r=-\infty}^{+\infty} \frac{X(s - j2r\omega_0)}{[(\tau s + 1) - j2r\omega_0]} \tag{85}$$

$$\left\{ \frac{1}{r} \tan \pi r - \frac{2\omega_0 \tau}{(\tau s + 1)} \tanh \frac{\pi}{2} \left(\frac{\tau s + 1}{\tau \omega_0} \right) \right\} \epsilon^{j2r\left(\phi - \frac{i-1}{N}\pi\right)} .$$

The crucial term in equation (85) with respect to harmonics is

$$\sum_{i=1}^{N} \epsilon^{j2r\left(\phi - \frac{i-1}{N}\pi\right)} .$$

Rewriting this term, we find that

$$\sum_{i=1}^{N} \epsilon^{j2r\left(\phi - \frac{i-1}{N}\pi\right)} = \epsilon^{j2r\phi} \sum_{i=1}^{N} \epsilon^{-j\frac{r}{N}(i-1)2\pi} . \tag{86}$$

This sum is a finite geometric series and will be zero for all values of r and N except where the ratio of r to N is an integer, or $\frac{r}{N} = k$. Therefore, for r = kN, where k takes on all integer values, equation (86) becomes

$$\epsilon^{j2kN\phi} \sum_{i=1}^{N} \epsilon^{-jk(i-1)2\pi} = N \epsilon^{j2kN\phi} . \tag{87}$$

By substituting r = kN into equation (85)

$$Y(s) = \frac{N\alpha}{\pi} \sum_{k=-\infty}^{+\infty} \frac{X(s - j2kN\omega_0)}{[(\tau s + 1) - j2kN\omega_0]} \cdot \left\{ \frac{1}{kN} \tan kN\pi \right.$$

$$\left. - \frac{2\omega_0 \tau}{(\tau s + 1)} \tanh \frac{\pi}{2} \left(\frac{\tau s + 1}{\tau \omega_0} \right) \right\} \epsilon^{j2kN\phi} . \tag{88}$$

The lowest harmonic present in the output of equation (88) will be for k = 1, the next lowest harmonic for k = -1, and so forth. A table can be made of the output harmonics as a function of N, as shown in Table I.

TABLE I. OUTPUT HARMONICS AS A FUNCTION OF NUMBER OF COMMUTATION FUNCTIONS

Number of Commutation Functions-N	Order of Harmonics								
	3rd	5th	7th	9th	11th	13th	15th	17th	19th
1	X	X	X	X	X	X	X	X	X
2	X	X	X	X	X	X	X	X	X
3		X	X		X	X		X	X
4			X	X			X	X	
5				X	X				X
6					X	X			
7						X	X		
8							X	X	

The effect of adding commutated capacitors, properly phased, can also be shown with a frequency spectrum graph as in Figure 34. The amplitudes shown are not to scale. Although a larger number of phases greatly reduce the lower order harmonics present in the CN output, it should be recognized that mechanization for the required commutation function may become increasingly complex. For example, one mechanization scheme using flip-flop circuits to obtain the desired phasing requires (2N-1) flip-flop circuits, where N is the number of phases. Therefore, doubling the number of phases almost doubles the required number of flip-flop circuits.

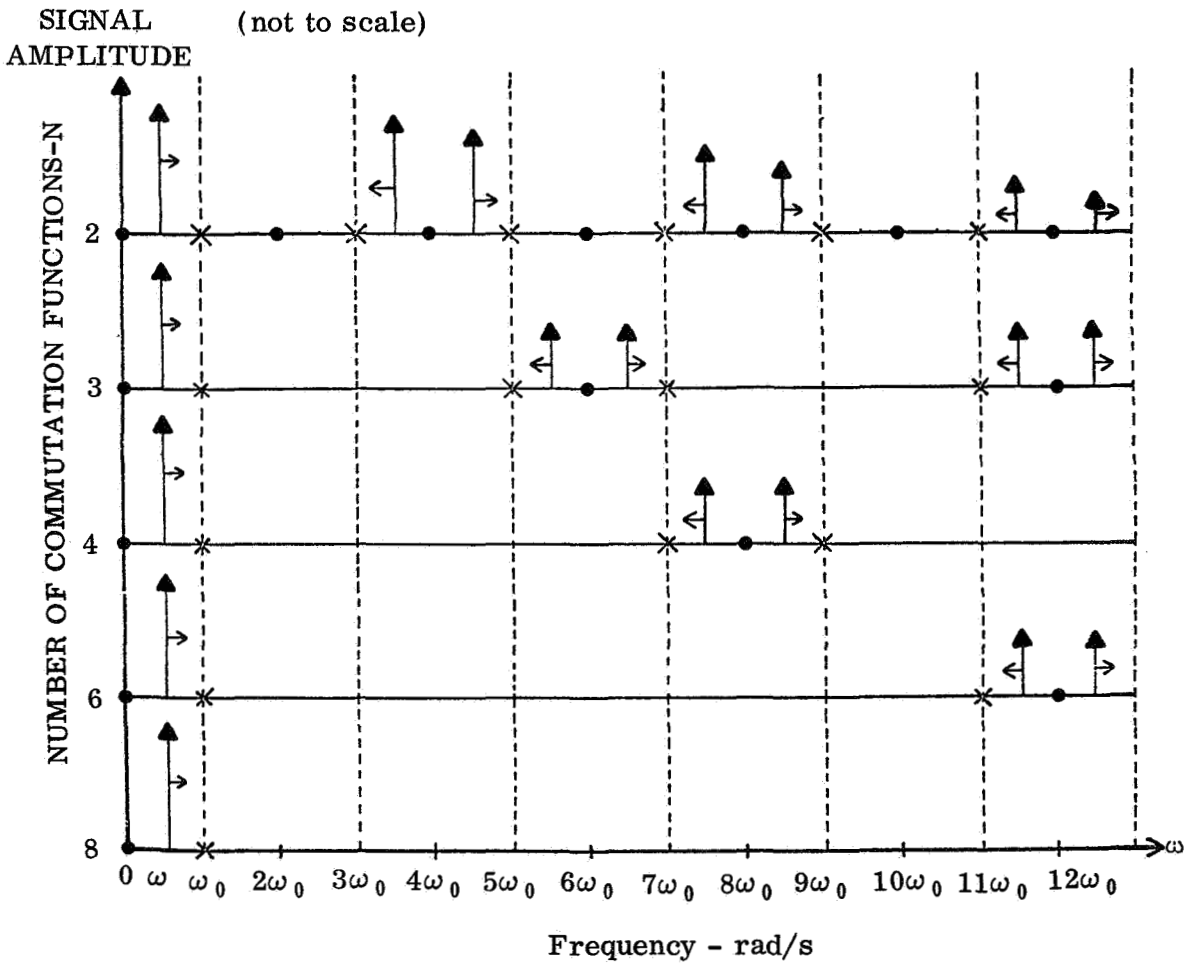

FIGURE 34. FREQUENCY SPECTRUM FOR POLYPHASE CN OUTPUT

ANALYSIS OF RC COMMUTATED NETWORKS WITH FEEDBACK

General

Before full utilization of CN's in control system applications can be expected, a solution to the problem of CN's with feedback loops must be realized. Commutation action always generates undesirable harmonics in the control loop and the assumption used in AC carrier control systems that the low-pass characteristic of the plant sufficiently attenuates all the harmonics generated by demodulation may not be adequate for stability considerations. It is essential, therefore, to provide a method of analyzing feedback control systems that includes the effects of all the harmonics generated by the CN's.

The analysis of a polyphase CN with feedback was first given by Carroll [15]. He solved the problem of an active, coupled CN with a constant-gain feedback element as shown in Figure 31(b). Analyses of an uncoupled polyphase CN with a constant-gain feedback element were given by Asner [13], Carroll [15], Lowry and Roan [14]. In this section, the analysis of CN's with generalized transfer functions as feedback elements will be presented for both coupled and uncoupled CN's. The technique used for this analysis is an extension to that developed by Carroll. A technique for treating a wide range of forward transfer functions used in this method of analysis is also presented.

Coupled Polyphase CN's with a Generalized Feedback Element

The generalized polyphase CN that will be used for this analysis is shown in Figure 35. Equation (38) for the single-capacitor CN is used to describe the i^{th} path of Figure 35.

$$Y_i(s) = -\frac{4}{\pi^2} \sum_{r=-\infty}^{\infty} Z(s - j2r\omega_0)\, \epsilon^{j2r\left(\phi - \frac{i-1}{N}\pi\right)}$$

$$\cdot \sum_{\substack{\ell=1 \\ \text{odd}}}^{\infty} \left\{ \frac{G(s - j\ell\omega_0)}{\ell\,(2r - \ell)} - \frac{G(s + j\ell\omega_0)}{\ell\,(2r + \ell)} \right\}. \qquad (89)$$

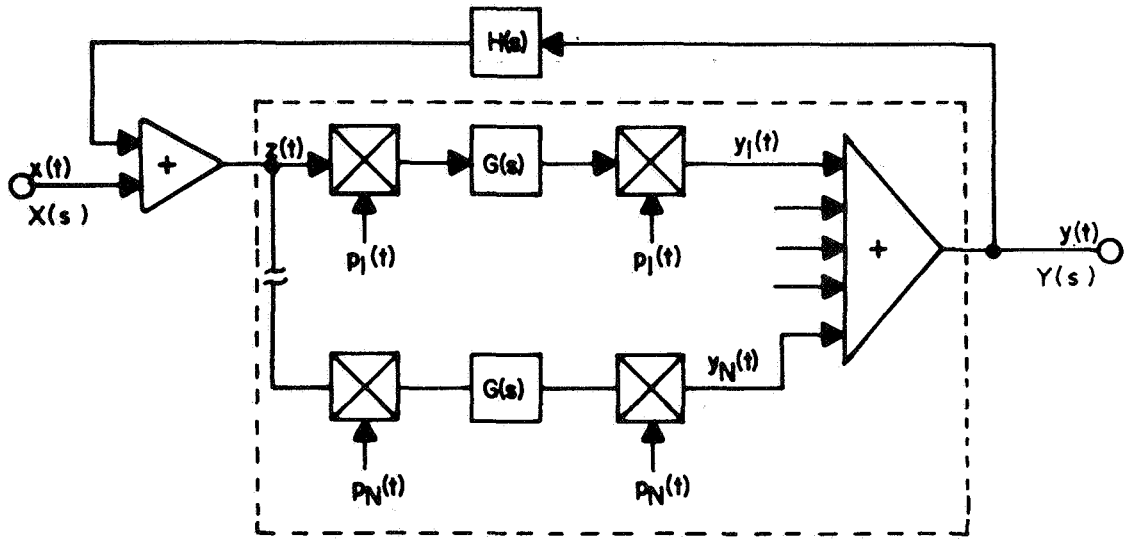

FIGURE 35. GENERALIZED POLYPHASE COUPLED CN WITH FEEDBACK

The symbols of equation (38) have been changed in equation (89) to correspond with those of Figure 35. To reduce equation (89) to a single infinite series, it is necessary to select a specific forward, noncommutated, transfer function G(s). The transfer function that was used earlier in this report is also used here,

$$G(s) = \frac{\alpha}{\tau s + 1} \quad . \tag{90}$$

This transfer function represents the active first order lag network shown in Figure 17, where α is $-\frac{R_1}{R_0}$ and τ is R_1C_1.

When equation (90) is substituted into equation (89), the second summation becomes

$$\sum_{\substack{\ell=1 \\ \text{odd}}}^{\infty} \frac{\alpha}{[\tau s + 1 - j\ell\tau\omega_0][2r - \ell]\ell} - \frac{\alpha}{[\tau s + 1 + j\ell\tau\omega_0][2r + \ell]\ell}$$

$$= -\frac{\frac{\alpha\pi}{4r}\tan \pi r - \frac{\alpha\tau\omega_0\pi}{2(\tau s + 1)}\tanh \frac{\pi}{2}\left(\frac{\tau s + 1}{\tau\omega_0}\right)}{[\tau s + 1 - j2r\tau\omega_0]} \quad . \tag{91}$$

By substituting equation (91) into equation (89)

$$Y_i(s) = \frac{\alpha}{\pi} \sum_{r=-\infty}^{+\infty} Z(s - j2r\omega_0)\, \epsilon^{j2r\left(\phi - \frac{i-1}{N}\pi\right)} \cdot \left\{ \frac{\frac{1}{r}\tan \pi r - \frac{2\tau\omega_0}{(\tau s+1)} \tanh \frac{\pi}{2}\left(\frac{\tau s+1}{\tau\omega_0}\right)}{[\tau s+1 - j2r\tau\omega_0]} \right\} . \tag{92}$$

Now summing the outputs of all N forward paths of the CN of Figure 35, we see that the total output will be

$$Y(s) = \frac{\alpha}{\pi} \sum_{i=1}^{N} \sum_{r=-\infty}^{+\infty} Z(s - j2r\omega_0)\, \epsilon^{j2r\left(\phi - \frac{i-1}{N}\pi\right)} \cdot \left\{ \frac{\frac{1}{r}\tan \pi r - \frac{2\tau\omega_0}{(\tau s+1)} \tanh \frac{\pi}{2}\left(\frac{\tau s+1}{\tau\omega_0}\right)}{[\tau s+1 - j2r\tau\omega_0]} \right\} . \tag{93}$$

This is the same as equation (85); therefore, when applying the same procedures, equation (93) reduces to

$$Y(s) = \frac{\alpha N}{\pi} \sum_{k=-\infty}^{+\infty} Z(s - j2kN\omega_0) \cdot \left\{ \frac{\frac{1}{kN}\tan kN\pi - \frac{2\tau\omega_0}{(\tau s+1)} \tanh \frac{\pi}{2}\left(\frac{\tau s+1}{\tau\omega_0}\right)}{[\tau s+1 - j2kN\tau\omega_0]} \right\} , \tag{94}$$

where k takes on all integers.

It has been shown that for polyphase CN's the frequency response was insensitive to the phase parameter ϕ in the frequency range of interest; that is, $\omega < N\omega_0$. Therefore, in equation (94), ϕ was omitted.

From Figure 35 the relation for $Z(s)$ can be written as

$$Z(s) = H(s)\ Y(s) + X(s). \tag{95}$$

By shifting the frequency of each term in equation (95) by $j2kN\omega_0$, we can write

$$\mathbf{Z}(s - j2kN\omega_0) = H(s - j2kN\omega_0)\ Y(s - j2kN\omega_0) + \mathbf{X}(s - j2kN\omega_0). \tag{96}$$

By substituting equation (96) into equation (94)

$$Y(s) = \frac{N\alpha}{\pi} \sum_{k=-\infty}^{+\infty} [Y(s - j2kN\omega_0)\ H(s - j2kN\omega_0) + X(s - j2kN\omega_0)]$$

$$\cdot \left\{ \frac{\frac{1}{kN} \tan kN\pi - \frac{2\tau\omega_0}{(\tau s + 1)} \tanh \frac{\pi}{2} \left(\frac{\tau s + 1}{\tau \omega_0} \right)}{[\tau s + 1 - j2kN\tau\omega_0]} \right\} . \tag{97}$$

For any specific value of k, other than $k = 0$, equation (97) would have two dependent variables, $Y(s)$ and $Y(s - j2kN\omega_0)$. It can therefore be reasoned that to solve equation (97) in terms of $Y(s)$ for any specific value of k, a second equation will be required. Let this second equation have the same form as equation (97) but be shifted in frequency by the amount $2mN\omega_0$, or

$$Y(s - j2mN\omega_0) = \frac{N\alpha}{\pi} \sum_{k=-\infty}^{+\infty} [\, Y(s - j2N\omega_0[\, k+m\,]\,)\; H(s - j2N\omega_0[\, k+m\,]\,)$$

$$+ X(s - j2N\omega_0[\, k+m\,]\,)\,] \left\{ \frac{\frac{1}{kN}\tan kN\pi - \frac{2\tau\omega_0 \tanh \frac{\pi}{2}\left(\frac{\tau s+1-j2mN\tau\omega_0}{\tau\omega_0}\right)}{(\tau s+1-j2mN\tau\omega_0)}}{[\tau s+1-j2N\omega_0\tau\,(k+m)]} \right\}, \tag{98}$$

where m is any integer except zero. In equation (98) let $k + m = \ell$; then equation (98) becomes

$$Y(s - j2mN\omega_0) = \frac{N\alpha}{\pi} \sum_{\ell=-\infty}^{+\infty} [\, Y(s - j2\ell N\omega_0)\; H(s - j2\ell N\omega_0) + X(s - j2\ell N\omega_0)]$$

$$\cdot \left\{ \frac{\frac{1}{N(\ell-m)}\tan\,(\ell-m)N\pi - \frac{2\tau\omega_0 \tanh \frac{\pi}{2}\left(\frac{\tau s+1}{\tau\omega_0}\right)}{(\tau s+1-j2mN\tau\omega_0)}}{(\tau s+1-j2\ell N\tau\omega_0)} \right\}, \tag{99}$$

because

$$\tanh \frac{\pi}{2}\left(\frac{\tau s+1-j2mN\tau\omega_0}{\tau\omega_0}\right) = \tanh \frac{\pi}{2}\left(\frac{\tau s+1}{\tau\omega_0}\right) .$$

If equation (97) is rewritten as

$$\left\{ Y(s) = \frac{N\alpha}{\pi} \left\{ [\, Y(s)\; H(s) + X(s)\,] \left[\frac{\pi(\tau s+1) - 2\tau\omega_0 \tanh \frac{\pi}{2}\left(\frac{\tau s+1}{\tau\omega_0}\right)}{(\tau s+1)^2} \right] \right. \right.$$

$$\left. + [\, Y(s - j2mN\omega_0)\; H(s - j2mN\omega_0) + X(s - j2mN\omega_0)\,] \right\}$$

$$\cdot \left[\frac{-2\tau\omega_0 \tanh \frac{\pi}{2}\left(\frac{\tau s+1}{\tau\omega_0}\right)}{(\tau s+1-j2mN\tau\omega_0)(\tau s+1)} \right] + \sum_{\substack{k=-\infty \\ k\neq 0,\ m}}^{+\infty} [\,Y(s-j2kN\omega_0)\,H(s-j2kN\omega_0)$$

$$+ X(s-j2kN\omega_0)] \left[\frac{-2\tau\omega_0 \tanh \frac{\pi}{2}\left(\frac{\tau s+1}{\tau\omega_0}\right)}{(\tau s+1-j2kN\tau\omega_0)(\tau s+1)} \right] \Bigg\}, \tag{100}$$

and equation (99) is rewritten as

$$Y(s-j2mN\omega_0) = \frac{N\alpha}{\pi} \Bigg\{ [\,Y(s)\,H(s) + X(s)] \left[\frac{-2\tau\omega_0 \tanh \frac{\pi}{2}\left(\frac{\tau s+1}{\tau\omega_0}\right)}{(\tau s+1-j2mN\tau\omega_0)(\tau s+1)} \right]$$

$$+ [\,Y(s-j2mN\omega_0)\;H(s-j2mN\omega_0) + X(s-j2mN\omega_0)]$$

$$\cdot \left[\frac{\pi(\tau s+1-j2mN\tau\omega_0) - 2\tau\omega_0 \tanh \frac{\pi}{2}\left(\frac{\tau s+1}{\tau\omega_0}\right)}{(\tau s+1-j2mN\tau\omega_0)^2} \right]$$

$$+ \sum_{\substack{\ell=-\infty \\ \ell\neq 0,\ m}}^{+\infty} [\,Y(s-j2\ell N\omega_0)\;H(s-j2\ell N\omega_0) + X(s-j2\ell N\omega_0)] \tag{101}$$

$$\cdot \left[\frac{-2\tau\omega_0 \tanh \frac{\pi}{2}\left(\frac{\tau s+1}{\tau\omega_0}\right)}{(\tau s+1-j2mN\tau\omega_0)(\tau s+1-j2\ell N\tau\omega_0)} \right] \Bigg\},$$

then equations (100) and (101) are seen to have similar terms but different coefficients. If equation (100) is multiplied by $[\tau s + 1]$ and equation (101) by $[\tau s + 1 - j2mN\tau\omega_0]$, then the terms of the infinite series in both equations are identical. By subtracting equation (101) from equation (100), after the above multiplication

$$Y(s)\,[\tau s + 1] - Y(s - j2mN\omega_0)\,[\tau s + 1 - j2mN\tau\omega_0]$$

$$= \frac{N\alpha}{\pi}\{[Y(s)\,H(s) + X(s)]\,(\pi) + [Y(s - j2mN\omega_0)\,H(s - j2mN\omega_0)$$

$$+ X(s - j2mN\omega_0)]\,(-\pi)\}\,. \tag{102}$$

Cancelling and regrouping terms, we see that

$$Y(s - j2mN\omega_0)\,([\tau s + 1 - j2mN\tau\omega_0] - N\alpha\,H(s - j2mN\omega_0))$$

$$= Y(s)\,(\tau s + 1 - N\alpha\,H(s)) - X(s)N\alpha + X(s - j2mN\omega_0)N\alpha \tag{103}$$

or

$$Y(s - j2mN\omega_0) = \frac{(\tau s + 1 - N\alpha\,H(s))\,Y(s) - N\alpha\,X(s) + N\alpha\,X(s - j2mN\omega_0)}{\tau s + 1 - j2mN\tau\omega_0 - N\alpha\,H(s - j2mN\omega_0)}. \tag{104}$$

By substituting equation (104) into equation (97), letting m = k, and regrouping terms

$$Y(s) = \frac{\left\{A(1 - B) + (N\alpha)^2 B \sum_{k=-\infty}^{+\infty}{}' \frac{H(s - j2kN\omega_0)}{C[C - N\alpha\,H(s - j2kN\omega_0)]}\right\} X(s)}{1 - A[1 - B]\,H(s) + (N\alpha)^2 B\left[\frac{1}{A} - H(s)\right]\sum_{k=-\infty}^{+\infty}{}' \frac{H(s - j2kN\omega_0)}{C[C - N\alpha\,H(s - j2kN\omega_0)]}}$$

$$- \frac{(N\alpha)\,B \sum_{k=-\infty}^{+\infty}{}' \frac{X(s - j2kN\omega_0)}{[C - N\alpha\,H(s - j2kN\omega_0)]}}{1 - A[1 - B]\,H(s) + (N\alpha)^2 B\left[\frac{1}{A} - H(s)\right]\sum_{k=-\infty}^{+\infty}{}' \frac{H(s - j2kN\omega_0)}{C[C - N\alpha\,H(s - j2kN\omega_0)]}}, \tag{105}$$

where

$$A = \frac{N\alpha}{\tau s + 1}$$

$$B = \frac{2\tau\omega_0 \tanh \frac{\pi}{2}\left(\frac{\tau s + 1}{\tau\omega_0}\right)}{\pi(\tau s + 1)}$$

$$C = \tau s + 1 - j2kN\tau\omega_0$$

$$\sum_{k=-\infty}^{+\infty}{}' = \text{sum of all k terms except k = 0.}$$

The output, Y(s), of the CN shown in Figure 35 is completely described by equation (105) in terms of the input signal, X(s), the feedback transfer function H(s), and the CN parameters. This expression is good for any transfer function H(s) in the feedback path and for any number of phases in a polyphase CN. For a different forward transfer function G(s) the same procedure would have to be followed to obtain an equivalent expression.

If the so-called "transfer function" of the CN is desired, then equation (105) is simplified by considering only the ratio of the fundamental signal frequency component in the output to that in the input, or

$$\frac{Y(s)}{X(s)} = \frac{A[1-B] + [N\alpha]^2 B \sum_{k=-\infty}^{+\infty}{}' \frac{H(s - j2kN\omega_0)}{C[C - N\alpha H(s - j2kN\omega_0)]}}{1 - A[1-B]H(s) + [N\alpha]^2 B\left[\frac{1}{A} - H(s)\right]\sum_{k=-\infty}^{+\infty}{}' \frac{H(s - j2kN\omega_0)}{C[C - N\alpha H(s - j2kN\omega_0)]}}. \tag{106}$$

This transfer function cannot be obtained by using linear feedback theory; for example, if k is set equal to zero in equation (88) then the open-loop transfer function of the CN is found to be

$$\frac{Y(s)}{X(s)} = A[1 - B], \tag{107}$$

where A and B are defined for equation (105).

For positive feedback, as was used in deriving equation (105), the closed-loop transfer function using linear theory would be

$$\frac{Y(s)}{X(s)} = \frac{A[1 - B]}{1 - A[1 - B]\ H(s)}\ , \tag{108}$$

where $H(s)$ is the transfer function of the feedback element.

It is obvious when equation (108) is compared to equation (106) that linear feedback theory does not apply to commutated networks because a non-linear signal generation effect results from the multiplication of the feedback harmonics or sideband signals with the commutation function at the input to the network.

Uncoupled Polyphase CN with a Generalized Feedback Element

The technique just shown for analyzing the coupled CN with a feedback circuit can also be applied to the uncoupled CN shown in Figure 36. A slightly different procedure will be necessary, however, because of the phasing term present in $Y_i(s)$. When using equation (89) and Figure 36, the equation for the i^{th} path can be written as

$$Y_i(s) = -\frac{4}{\pi^2} \sum_{r=-\infty}^{+\infty} Z_i(s - j2r\omega_0)\, \epsilon^{j2r\left(\phi - \frac{i-1}{N}\pi\right)} \sum_{\substack{\ell=-\infty \\ \text{odd}}}^{+\infty} \frac{G(s - j\ell\omega_0)}{\ell(2r - \ell)}\ . \tag{109}$$

For the uncoupled case considered here, $Z_i(s - j2r\omega_0)$ can be expressed as

$$Z_i(s - j2r\omega_0) = X(s - j2r\omega_0) + Y_i(s - j2r\omega_0)\, H(s - j2r\omega_0)\,. \tag{110}$$

By substituting equation (110) into equation (109)

$$Y_i(s) = -\frac{4}{\pi^2} \sum_{r=-\infty}^{+\infty} X(s - j2r\omega_0)\, \epsilon^{-j2r\pi \frac{i-1}{N}} \sum_{\substack{\ell=-\infty \\ \text{odd}}}^{+\infty} \frac{G(s - j\ell\omega_0)}{\ell(2r-\ell)}$$

$$- \frac{4}{\pi^2} \sum_{r=-\infty}^{+\infty} Y_i(s - j2r\omega_0)\, H(s - j2r\omega_0) \epsilon^{-j2r\pi \frac{i-1}{N}} \sum_{\substack{\ell=-\infty \\ \text{odd}}}^{+\infty} \frac{G(s-j\ell\omega_0)}{\ell(2r-\ell)} \,, \tag{111}$$

where the phase angle ϕ has been set equal to zero. It was shown that for a polyphase CN, ϕ was not a significant factor for $\omega < N\omega_0$. For this derivation, ω will be considered to be less than $N\omega_0$.

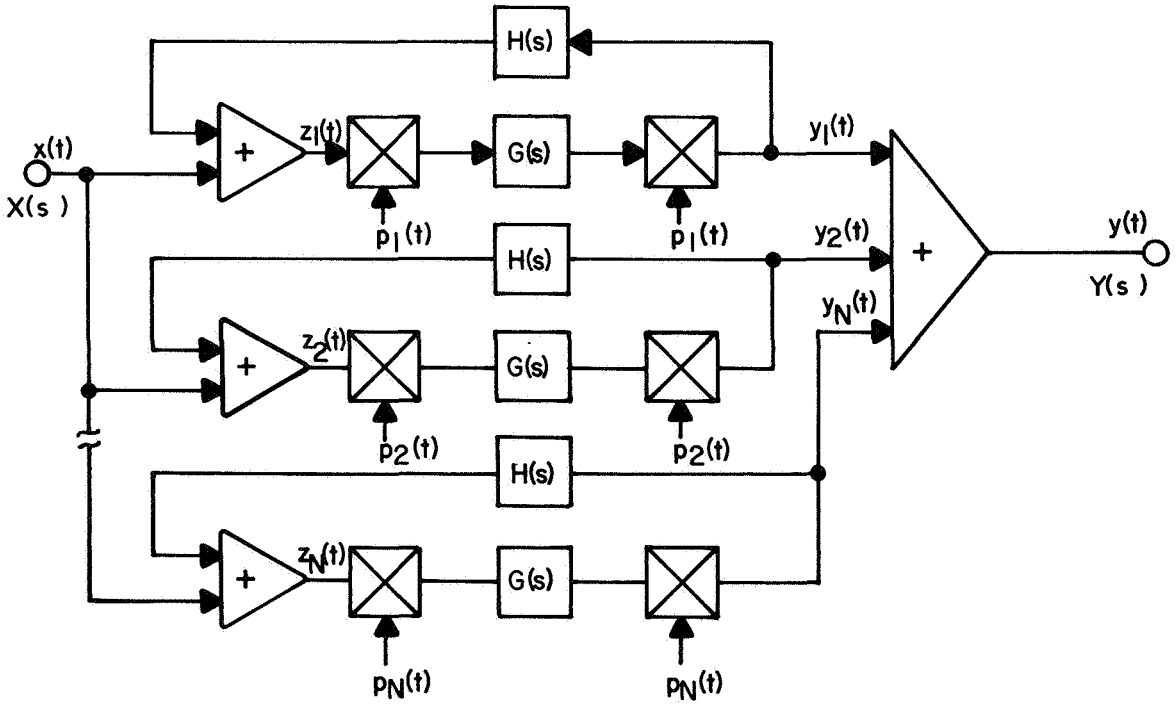

FIGURE 36. GENERALIZED POLYPHASE UNCOUPLED CN

To solve for $Y_i(s)$ in terms of the input $X(s)$, the same initial step used for the coupled case is used. The frequency shifted expression for $Y_i(s)$ is

$$Y_i(s - j2m\omega_0) = -\frac{4}{\pi^2} \sum_{r=-\infty}^{+\infty} X(s - j2\omega_0[r+m])\, \epsilon^{-j2r\pi\frac{i-1}{N}} \sum_{\substack{\ell=-\infty \\ \text{odd}}}^{+\infty} \frac{G(s-j\omega_0[\ell+2m])}{\ell(2r-\ell)}$$

$$-\frac{4}{\pi^2} \sum_{r=-\infty}^{+\infty} Y_i(s - j2\omega_0[r+m])\, H(s - j2\omega_0[r+m])\, \epsilon^{-j2r\pi\frac{i-1}{N}}$$

$$\cdot \sum_{\ell=-\infty}^{+\infty} \frac{G(s - j\omega_0[\ell + 2m])}{\ell(2r-\ell)} \quad , \tag{112}$$

where m is any integer except zero. By rewriting equation (111) with the $r = 0$ and $r = m$ terms extracted from under the r summation sign

$$-\frac{\pi^2}{4} Y_i(s) = X(s) \sum_{\substack{\ell=-\infty \\ \text{odd}}}^{+\infty} \frac{G(s-j\ell\omega_0)}{-\ell^2} + X(s-j2m\omega_0)\epsilon^{-j2m\pi\frac{i-1}{N}} \sum_{\substack{\ell=-\infty \\ \text{odd}}}^{+\infty} \frac{G(s-j\ell\omega_0)}{\ell(2m-\ell)}$$

$$+ \sum_{\substack{r=-\infty \\ r\neq 0 \\ r\neq m}}^{+\infty} X(s - j2r\omega_0)\, \epsilon^{-j2r\pi\frac{i-1}{N}} \sum_{\substack{\ell=-\infty \\ \text{odd}}}^{+\infty} \frac{G(s - j\ell\omega_0)}{\ell(2r-\ell)} + Y_i(s)\, H(s) \sum_{\substack{\ell=-\infty \\ \text{odd}}}^{+\infty} \frac{G(s-j\ell\omega_0)}{-\ell^2}$$

$$+ Y_i(s - j2m\omega_0)\, H(s - j2m\omega_0)\, \epsilon^{-j2m\pi\frac{i-1}{N}} \sum_{\substack{\ell=-\infty \\ \text{odd}}}^{+\infty} \frac{G(s - j\ell\omega_0)}{\ell(2m-\ell)}$$

$$+ \sum_{\substack{r=-\infty \\ r\neq 0 \\ r\neq m}}^{+\infty} Y_i(s - j2r\omega_0)\, H(s - j2r\omega_0)\, \epsilon^{-j2r\pi\frac{i-1}{N}} \sum_{\substack{\ell=-\infty \\ \text{odd}}}^{+\infty} \frac{G(s - j\ell\omega_0)}{\ell(2r-\ell)} . \tag{113}$$

Before rewriting equation (112), let $r + m = k$; then extract the terms for $k = 0$ and $k = m$ from under the k summation sign to give

$$-\frac{\pi^2}{4} Y_i(s - j2m\omega_0) = X(s)\ \epsilon^{j2m\pi\frac{i-1}{N}} \sum_{\substack{\ell=-\infty \\ \text{odd}}}^{+\infty} \frac{G(s - j\omega_0[\ell + 2m])}{-\ell(\ell + 2m)}$$

$$+ X(s - j2m\omega_0) \sum_{\substack{\ell=-\infty \\ \text{odd}}}^{+\infty} \frac{G(s - j\omega_0[\ell + 2m])}{-\ell^2}$$

$$+ \sum_{\substack{k=-\infty \\ k\neq 0 \\ k\neq m}}^{+\infty} X(s - j2k\omega_0) \cdot \epsilon^{-j2\pi(k-m)\frac{i-1}{N}} \sum_{\substack{\ell=-\infty \\ \text{odd}}}^{+\infty} \frac{G(s - j\omega_0[\ell + 2m])}{\ell(2k - [\ell + 2m])}$$

$$+ Y_i(s)\, H(s)\, \epsilon^{j2\pi m\frac{i-1}{N}} \cdot \sum_{\substack{\ell=-\infty \\ \text{odd}}}^{+\infty} \frac{G(s - j\omega_0[\ell + 2m])}{-\ell(\ell + 2m)}$$

$$+ Y_i(s - j2\omega_0 m)\, H(s - j2\omega_0 m) \sum_{\substack{\ell=-\infty \\ \text{odd}}}^{+\infty} \frac{G(s - j\omega_0[\ell + 2m])}{-\ell^2}$$

$$+ \sum_{\substack{k=-\infty \\ k\neq 0 \\ k\neq m}}^{+\infty} Y_i(s - j2k\omega_0)\, H(s - j2k\omega_0) \cdot \epsilon^{-j2\pi(k-m)\frac{i-1}{N}} \sum_{\substack{\ell=-\infty \\ \text{odd}}}^{+\infty} \frac{G(s - j\omega_0[\ell + 2m])}{\ell(2k - [\ell + 2m])}. \quad (114)$$

It is now necessary to use a specific transfer function for G(s) to solve equations (113) and (114) in terms of $Y_i(s)$. The same transfer function used to solve the coupled case ($G(s) = \frac{\alpha}{\tau s + 1}$) will be used. Making the appropriate

substitution in equations (113) and (114) for G(s) and the frequency shifted G(s), then multiplying equation (113) by $(\tau s + 1)\ \epsilon^{j2\pi m(i-1)/N}$ and equation (114) by $(\tau s \quad 1 - j2m\tau\omega_0)$, and then subtracting equation (114) from equation (113), we find that

$$
\begin{aligned}
&-\frac{\pi^2}{4}\ Y_i(s)\,(\tau s+1)\,\epsilon^{j2\pi m\,\frac{i-1}{N}} + \frac{\pi^2}{4}\ Y_i(s-j2m\omega_0)\,(\tau s+1-j2m\tau\omega_0)\\
&= X(s)\,\{A\}\,(\tau s+1)\,\epsilon^{j2\pi m\,\frac{i-1}{N}} + X(s-j2m\omega_0)\,\{B\}\,(\tau s+1)\\
&+ \sum_{\substack{r=-\infty\\ r\neq 0,\ m}}^{+\infty} X(s-j2r\omega_0)\,\epsilon^{-j2\pi(r-m)\,\frac{i-1}{N}}\,\{C\}\,(\tau s+1)\\
&+ Y_i(s)\,H(s)\,\{A\}\,(\tau s+1)\,\epsilon^{j2\pi m\,\frac{i-1}{N}} + Y_i(s-j2m\omega_0)\,H(s-j2m\omega_0)\{B\}\,(\tau s+1)\\
&+ \sum_{\substack{r=-\infty\\ r\neq 0,\ m}}^{+\infty} Y_i(s-j2r\omega_0)\,H(s-j2r\omega_0)\{C\}\,(\tau s+1)\,\epsilon^{-j2\pi(r-m)\,\frac{i-1}{N}}\\
&- X(s)\{D\}\,(\tau s+1-j2m\tau\omega_0)\epsilon^{j2m\,\frac{i-1}{N}\pi} - X(s-j2m\omega_0)\{E\}\,(\tau s+1-j2m\tau\omega_0)\\
&- \sum_{\substack{k=-\infty\\ k\neq 0,\ m}}^{+\infty} X(s-j2k\omega_0)\,\{F\}\,(\tau s+1-j2m\tau\omega_0)\,\epsilon^{-j2\pi(k-m)\,\frac{i-1}{N}}\\
&- Y_i(s)\,H(s)\{D\}\,(\tau s+1-j2m\tau\omega_0)\epsilon^{j2\pi m\frac{i-1}{N}} - Y_i(s-j2m\omega_0)\,H(s-j2m\omega_0)\{E\}\\
&\qquad\qquad (\tau s+1-j2m\tau\omega_0)\\
&- \sum_{\substack{k=-\infty\\ k\neq 0,\ m}}^{+\infty} Y_i(s-j2k\omega_0)\,H(s-j2k\omega_0)\{F\}\,(\tau s+1-j2m\tau\omega_0)\,\epsilon^{-j2\pi(k-m)\,\frac{i-1}{N}}\ ,
\end{aligned}
\tag{115}
$$

where the symbols $\{A\}$, $\{B\}$, ... are denoted in Table II. Combining like terms in equation (115), we see that

$$
\begin{aligned}
&-\frac{\pi^2}{4} Y_i(s)(\tau s+1)\,\epsilon^{j2\pi m\frac{i-1}{N}} + \frac{\pi^2}{4} Y_i(s-j2m\omega_0)(\tau s+1-j2m\tau\omega_0) \\
&= X(s)\,\epsilon^{j2m\pi\frac{i-1}{N}}\,[\{A\}(\tau s+1) - \{D\}(\tau s+1-j2m\tau\omega_0)] \\
&+ X(s-j2m\omega_0)\,[\{B\}(\tau s+1) - \{E\}(\tau s+1-j2m\tau\omega_0)] \\
&+ \sum_{\substack{r=-\infty \\ r\neq 0,\ m}}^{+\infty} X(s-j2r\omega_0)[\{C\}(\tau s+1) - \{F\}(\tau s+1-j2m\tau\omega_0)]\,\epsilon^{-j2\pi(r-m)\frac{i-1}{N}} \\
&+ Y_i(s)\,H(s)\,[\{A\}(\tau s+1) - \{D\}(\tau s+1-j2m\tau\omega_0)]\,\epsilon^{j2\pi m\frac{i-1}{N}} \\
&+ Y_i(s-j2m\omega_0)\,H(s-j2m\omega_0)[\{B\}(\tau s+1) - \{E\}\ (\tau s+1\,0 j2m\tau\omega_0)] \\
&+ \sum_{\substack{r=-\infty \\ r\neq 0,\ m}}^{+\infty} Y_i(s-j2m\omega_0)\,H(s-j2m\omega_0)[\{C\}(\tau s+1) - \{F\}(\tau s+1-j2m\tau\omega_0)] \\
&\qquad \epsilon^{-j2\pi(r-m)\frac{i-1}{N}} \,. \qquad (116)
\end{aligned}
$$

The terms in each bracket can be evaluated as

$$
\begin{aligned}
[\{A\}(\tau s+1) - \{D\}\ (\tau s+1-j2m\tau\omega_0)] &= -\frac{\propto \pi^2}{4} \\
[\{B\}(\tau s+1) - \{E\}\ (\tau s+1-j2m\tau\omega_0)] &= \frac{\propto \pi^2}{4} \\
[\{C\}(\tau s+1) - \{F\}\ (\tau s+1-j2m\tau\omega_0)] &= 0\,.
\end{aligned}
$$

By substituting these values into equation (116)

TABLE II. ABBREVIATIONS USED IN EQUATION 115

No.	General Expression	For $G(s) = \frac{\alpha}{\tau s+1}$	Symbol In Equation 115
1	$\sum_{\ell=-\infty}^{+\infty}{}^{\text{odd}} \frac{G(s-j\ell\omega_0)}{-\ell^2}$	$-\frac{\alpha\pi^2}{4(\tau s+1)} + \frac{\alpha\pi\tau\omega_0}{2(\tau s+1)^2} \tanh\frac{\pi}{2}\left(\frac{\tau s+1}{\tau\omega_0}\right)$	{A}
2	$\sum_{\ell=-\infty}^{+\infty}{}^{\text{odd}} \frac{G(s-j\ell\omega_0)}{\ell(2m-\ell)}$	$\frac{\alpha\pi\tau\omega_0 \tanh\frac{\pi}{2}\left(\frac{\tau s+1}{\tau\omega_0}\right)}{2(\tau s+1)(\tau s+1-j2m\tau\omega_0)}$	{B}
3	$\sum_{\ell=-\infty}^{+\infty}{}^{\text{odd}} \frac{G(s-j\ell\omega_0)}{\ell(2r-\ell)}$	$\frac{-\frac{\alpha\pi}{4r}\tan\pi r + \frac{\alpha\pi\tau\omega_0}{2(\tau s+1)}\tanh\frac{\pi}{2}\left(\frac{\tau s+1}{\tau\omega_0}\right)}{(\tau s+1-j2r\tau\omega_0)}$	{C}
4	$\sum_{\ell=-\infty}^{+\infty}{}^{\text{odd}} \frac{G(s-j\omega_0[2m+\ell])}{-\ell(2m+\ell)}$	$\frac{\alpha\pi\tau\omega_0 \tanh\frac{\pi}{2}\left(\frac{\tau s+1}{\tau\omega_0}\right)}{2(\tau s+1)(\tau s+1-j2m\tau\omega_0)}$	{D}
5	$\sum_{\ell=-\infty}^{+\infty}{}^{\text{odd}} \frac{G(s-j\omega_0[2m+\ell])}{-\ell^2}$	$-\frac{\alpha\pi^2}{4(\tau s+1-j2m\tau\omega_0)} + \frac{\alpha\pi\tau\omega_0 \tanh\frac{\pi}{2}\left(\frac{\tau s+1}{\tau\omega_0}\right)}{2(\tau s+1-j2m\tau\omega_0)}$	{E}
6	$\sum_{\ell=-\infty}^{+\infty}{}^{\text{odd}} \frac{G(s-j\omega_0[2m+\ell])}{\ell(2k-[2m+\ell])}$	$\frac{\frac{\alpha\pi\tan\pi(k-m)}{4(k-m)} + \frac{\alpha\pi\tau\omega_0\tanh\frac{\pi}{2}\left(\frac{\tau s+1}{\tau\omega_0}\right)}{2(\tau s+1-j2m\tau\omega_0)}}{(\tau s+1-j2k\tau\omega_0)}$	{F}

NOTE: $\tanh\frac{\pi}{2}\left(\frac{\tau s+1-j2m\tau\omega_0}{\tau\omega_0}\right) = \tanh\frac{\pi}{2}\left(\frac{\tau s+1}{\tau\omega_0}\right)$.

$$-\frac{\pi^2}{4}\,Y_i(s)\,(\tau s+1)\epsilon^{j2\pi m\frac{i-1}{N}}+\frac{\pi^2}{4}\,Y_i(s-j2m\omega_0)\,(\tau s+1-j2m\tau\omega_0)$$

$$=X(s)\left[-\frac{\propto\pi^2}{4}\right]\epsilon^{j2\pi m\frac{i-1}{N}}+X(s-j2m\omega_0)\left[\frac{\propto\pi^2}{4}\right]$$

$$+\,Y_i(s)\,H(s)\left[-\frac{\propto\pi^2}{4}\right]\epsilon^{j2\pi m\frac{i-1}{N}}+Y_i(s-j2m\omega_0)\,H(s-j2m\omega_0)\left[\frac{\propto\pi^2}{4}\right]. \qquad (117)$$

By combining terms and solving for $Y_i(s - j2m\omega_0)$

$$Y_i(s-j2m\omega_0)=\frac{[\tau s+1-\propto H(s)]\,Y_i(s)\epsilon^{j2\pi m\frac{i-1}{N}}-\propto X(s)\epsilon^{j2\pi m\frac{i-1}{N}}+\propto X(s-j2m\omega_0)}{\tau s+1-j2m\tau\omega_0-\propto H(s-j2m\omega_0)} \qquad (118)$$

If equation (118) is compared with equation (104) for the coupled case, it will be seen that the equations are similar. Equation (104) represents the entire CN and therefore contains a factor N, the number of forward parallel paths in the equivalent block diagram. Equation (118) represents only a single i^{th} path and therefore contains the phasing term $\epsilon^{j2\pi m(i-1)/N}$.

To obtain Y(s) for the CN of Figure 36 it is necessary to substitute equation (118) into equation (115) to eliminate the frequency shifted values of $Y_i(s)$, and then to sum the $Y_i(s)$'s over all the forward paths. Performing the first step, we see that

$$Y_i(s)=\frac{4}{\pi^2}\,\{X(s)+Y_i(s)\,H(s)\}\left\{\frac{\propto\pi^2}{4(\tau s+1)}-\frac{\propto\pi\tau\omega_0}{2(\tau s+1)^2}\,\tanh\frac{\pi}{2}\left(\frac{\tau s+1}{\tau\omega_0}\right)\right\}$$

$$-\frac{4}{\pi^2}\sum_{r=-\infty}^{+\infty}{}'X(s-j2r\omega_0)\left[\frac{\propto\pi\tau\omega_0\tanh\frac{\pi}{2}\left(\frac{\tau s+1}{\tau\omega_0}\right)}{2(\tau s+1)\,(\tau s+1-j2r\tau\omega_0)}\right]\epsilon^{-j2\pi r\frac{i-1}{N}}$$

$$-\frac{4}{\pi^2}\sum_{r=-\infty}^{+\infty}{}' \left\{ \frac{[\tau s+1-\alpha H(s)]\, Y_i(s)\epsilon^{j2\pi r\frac{i-1}{N}} - \alpha X(s)\epsilon^{j2\pi r\frac{i-1}{N}} + \alpha X(s-j2r\omega_0)}{\tau s+1-j2r\tau\omega_0 - \alpha H(s-j2r\omega_0)} \right\}$$

$$\cdot \left\{ H(s-j2r\omega_0)\left[\frac{\alpha\pi\tau\omega_0 \tanh\frac{\pi}{2}\left(\frac{\tau s+1}{\tau\omega_0}\right)}{2(\tau s+1)(\tau s+1-j2r\tau\omega_0)} \right] \right\} \epsilon^{-j2\pi r\frac{i-1}{N}}. \tag{119}$$

Equation (119) can be simplified by letting

$$A = \frac{N\alpha}{\tau s+1}$$

$$B = \frac{2\omega_0\tau \tanh\frac{\pi}{2}\left(\frac{\tau s+1}{\tau\omega_0}\right)}{\pi(\tau s+1)}$$

$$C = \tau s+1-j2kN\tau\omega_0$$

$$\sum_{k=-\infty}^{+\infty}{}' = \text{sum of all k terms except } k=0$$

N = the number of forward paths in the equivalent block diagram.

Then substituting these expressions into equation (119), combining terms, and solving for $Y_i(s)$, we see that

$$Y_i(s) = \frac{\left\{ \frac{A}{N} - \frac{AB}{N} + \alpha^2 B \sum_{r=-\infty}^{+\infty}{}' \frac{H(s-j2r\omega_0)}{C[C-\alpha H(s-j2r\omega_0)]} \right\} X(s)}{1-\left[\frac{A}{N}-\frac{AB}{N}\right]H(s)+\alpha B\left[\frac{\alpha N}{A}-\alpha H(s)\right]\sum_{r=-\infty}^{+\infty}{}' \frac{H(s-j2r\omega_0)}{C[C-\alpha H(s-j2r\omega_0)]}}$$

$$- \frac{\alpha B \sum_{r=-\infty}^{+\infty}{}' \frac{X(s-j2r\omega_0)\,\epsilon^{-j2\pi r\frac{i-1}{N}}}{[C-\alpha H(s-j2r\omega_0)]}}{1-\left[\frac{A}{N}-\frac{AB}{N}\right]H(s)+\alpha B\left[\frac{\alpha N}{A}-\alpha H(s)\right]\sum_{r=-\infty}^{+\infty}{}' \frac{H(s-j2r\omega_0)}{C[C-\alpha H(s-j2r\omega_0)]}} \tag{120}$$

Equation (120) is summed over all N forward paths to obtain the total output

$$Y(s) = \sum_{i=1}^{N} Y_i(s) \ . \tag{121}$$

After performing the indicated summation in equation (121), we can see that the only harmonics present in the output will be when the ratio $\frac{r}{N} = k$, where k is an integer. Substituting equation (120) into equation (121), letting $r = kN$, and then performing the indicated summation, we find that

$$Y(s) = \frac{\left\{A[1-B] + N\alpha^2 B \sum_{k=-\infty}^{+\infty}{}' \frac{H(s - j2kN\omega_0)}{C[C - \alpha H(s - j2kN\omega_0)]}\right\}}{1 - \frac{A}{N}[1-B]\,H(s) + \alpha^2 B\left[\frac{N}{A} - H(s)\right]\sum_{k=-\infty}^{+\infty}{}' \frac{H(s - j2kN\omega_0)}{C[C - \alpha H(s - j2kN\omega_0)]}} X(s)$$

$$- \frac{\alpha NB \sum_{k=-\infty}^{+\infty}{}' \frac{X(s - j2kN\omega_0)}{[C - \alpha H(s - j2kN\omega_0)]}}{1 - \frac{A}{N}[1-B]\,H(s) + \alpha^2 B\left[\frac{N}{A} - H(s)\right]\sum_{k=-\infty}^{+\infty}{}' \frac{H(s - j2kN\omega_0)}{C[C - \alpha H(s - j2kN\omega_0)]}} \ . \tag{122}$$

The output, Y(s), of the uncoupled CN of Figure 36 is completely characterized by equation (122). For the case of $N = 1$, we see that equations (105) and (122) are identical, or the coupled case is the same as the uncoupled case for a single commutated capacitor. For $N > 1$, the uncoupled configuration (Fig. 36) reduces the effect of the feedback transfer function H(s) and the frequency shifted transfer function $H(s - j2kN\omega_0)$ by a factor of N from that of the coupled case. This condition results in an increase in the magnitude of the harmonics or sideband frequency components. These results, deduced from equation (122), have also been observed experimentally.

It would be highly desirable if the output of the CN, Y(s), could be expressed as a function of a generalized forward transfer function G(s) as well

as a generalized feedback transfer function H(s). However, this does not appear to be possible with the technique just presented. One of the important steps in solving for Y(s) was to eliminate the dependent variable in its shifted form, $Y(s - j2kN\omega_0)$. This step was accomplished by modifying the coefficients of the terms still under the summation sign of both expressions (all terms except k = 0 and k = m) so that they would add out when the difference was taken between Y(s) and $Y(s - j2kN\omega_0)$. To perform the modification, each equation of Y(s) and $Y(s - j2kN\omega_0)$ was multiplied by a different factor dependent upon G(s) to insure the equality of the terms under the two infinite summation signs. This dependence upon G(s) appears to rule out any further generalization.

Forward Transfer Functions for Commutated Networks

In the analysis of CN's with a generalized feedback element, treated in the preceding two sections, a definite forward transfer function had to be specified to facilitate the calculation of the output, Y(s). Because of this requirement, a procedure for handling a wide range of forward transfer functions will now be given. The specific problem is to reduce the second infinite summation in equation (89) to a closed-form expression. The second infinite summation for a CN using square-wave commutation and a general forward transfer function G(s) is

$$\sum_{\substack{\ell=-\infty \\ \text{odd}}}^{+\infty} \frac{G(s - j\ell\omega_0)}{\ell(2r - \ell)} \quad . \tag{123}$$

The closed form expression of equation (123) for a forward transfer function $G(s) = \frac{\alpha}{\tau s + 1}$ has already been given and is listed in Table III. For cases where the forward transfer function is higher than a first order transfer function, but with nonrepeated roots, the same technique can be applied after expanding the transfer function into partial fractions. For example, let

$$G(s) = \frac{K}{(\tau_1 s + 1)(\tau_2 s + 1)} \quad , \tag{124}$$

where

$$\tau_1 \neq \tau_2 \, .$$

TABLE III. CLOSED FORMS FOR ELEMENTARY COMMUTATED TRANSFER FUNCTIONS

$G(s)$	$\sum_{\substack{\ell=-\infty \\ \text{odd}}}^{+\infty} \frac{G(s - j\ell\omega_0)}{\ell(2r-\ell)}$
$\frac{1}{\tau s}$	$-\frac{\pi \tan \pi r}{4r(\tau s - j2r\tau\omega_0)} + \frac{\pi\omega_0 \tanh \frac{\pi s}{2\omega_0}}{2\tau s(\tau s - j2r\tau\omega_0)}$
$\frac{\propto}{\tau s+1}$	$-\frac{\propto\pi \tan \pi r}{4r(\tau s+1-j2r\tau\omega_0)} + \frac{\propto\pi\tau\omega_0 \tanh \frac{\pi}{2}\left(\frac{\tau s+1}{\tau\omega_0}\right)}{2(\tau s+1)(\tau s+1-j2r\tau\omega_0)}$
$\frac{\propto}{(\tau s+1)^2}$	$-\frac{\propto\delta(r)}{(\tau s+1)^2} - \frac{\propto\pi^2 \operatorname{sech}^2 \frac{\pi}{2}\left(\frac{\tau s+1}{\tau\omega_0}\right)}{4(\tau s+1)(\tau s+1-j2r\tau\omega_0)}$ $+\frac{\propto\pi\tau\omega_0(\tau s+1-jr\tau\omega_0) \tanh \frac{\pi}{2}\left(\frac{\tau s+1}{\tau\omega_0}\right)}{(\tau s+1)^2(\tau s+1-j2r\tau\omega_0)^2}$
$\frac{\propto s}{\tau s+1}$	$-\frac{\propto\pi \tan \pi r\,[s(\tau s+1)+4\tau\omega_0^2 r^2 - j2r\omega_0]}{4r[(\tau s+1)^2+4r^2\tau^2\omega_0^2]}$ $-\frac{\propto\pi\omega_0 \tanh \frac{\pi}{2}\left(\frac{\tau s+1}{\tau\omega_0}\right)}{2(\tau s+1)(\tau s+1-j2r\tau\omega_0)}$
$\frac{\propto}{\tau^2 s^2+2\zeta\tau s+1}$ $(\zeta \neq 1)$	$\frac{\frac{\propto\pi}{2\sqrt{\zeta^2-1}}\left(\frac{\tan \pi r}{4r} - \frac{\omega_0 \tanh \frac{\pi}{2}\left(\frac{\tau s+\zeta+\sqrt{\zeta^2-1}}{\tau\omega_0}\right)}{2(\tau s+\zeta+\sqrt{\zeta^2-1})}\right)}{\tau s+\zeta+\sqrt{\zeta^2-1} - j2r\tau\omega_0}$ $-\frac{\frac{\propto\pi}{2\sqrt{\zeta^2-1}}\left(\frac{\tan \pi r}{4r} - \frac{\omega_0 \tanh \frac{\pi}{2}\left(\frac{\tau s+\zeta-\sqrt{\zeta^2-1}}{\tau\omega_0}\right)}{2(\tau s+\zeta-\sqrt{\zeta^2-1})}\right)}{\tau s+\zeta-\sqrt{\zeta^2-1} - j2r\tau\omega_0}$
	$\delta(r) = 1$ when $r = 0$ $\delta(r) = 0$ when $r \neq 0$

The partial fraction expansion is

$$G(s) = \frac{C_1}{\tau_1 s + 1} + \frac{C_2}{\tau_2 s + 1} \tag{125}$$

where

$$C_1 = \frac{K}{1 - \tau_2/\tau_1}$$

$$C_2 = \frac{K}{1 - \tau_1/\tau_2} \ .$$

Substituting equation (125) into expression (123) yields

$$\sum_{\substack{\ell = -\infty \\ \text{odd}}}^{+\infty} \left[\frac{C_1}{\ell(2r - \ell)\,(\tau_1 s + 1 - j\tau_1 \ell \omega_0)} + \frac{C_2}{\ell(2r - \ell)\,(\tau_2 s + 1 - j\tau_2 \ell \omega_0)} \right] . \tag{126}$$

Rearranging the terms of (126) to sum over positive integers only gives

$$\sum_{\substack{\ell = 1 \\ \text{odd}}}^{+\infty} \left[\frac{2C_1(\tau_1 s + 1 + j2r\tau_1\omega_0)}{(4r^2 - \ell^2)\ [(\tau_1 s + 1)^2 + \ell^2 \tau_1^2 \omega_0^2]} + \frac{2C_2(\tau_2 s + 1 + j2r\tau_2\omega_0)}{(4r^2 - \ell^2)\ [(\tau_2 s + 1)^2 + \ell^2 \tau_2^3 \omega_0^2]} \right] . \tag{127}$$

By using the identities from Appendix B, expression (127) can be written as

$$\left[\frac{-C_1 \left\{ \frac{\pi}{4r} \tan \pi r - \frac{2\tau_1\omega_0}{(\tau_1 s + 1)} \tanh \frac{\pi}{2} \left(\frac{\tau_1 s + 1}{\tau_1 \omega_0} \right) \right\}}{\tau_1 s + 1 - j2r\tau_1\omega_0} \right.$$

$$\left. - \frac{C_2 \left\{ \frac{\pi}{4r} \tan \pi r - \frac{2\tau_2\omega_0}{(\tau_2 s + 1)} \tanh \frac{\pi}{2} \left(\frac{\tau_2 s + 1}{\tau_2 \omega_0} \right) \right\}}{\tau_2 s + 1 - j2r\tau_2\omega_0} \right] . \tag{128}$$

The expression (128) can now be substituted into the equation for $Y_i(s)$, i.e., equation (89) for the coupled case, or equation (109) for the uncoupled case. An equivalent block diagram for G(s) after the partial fraction expansion has been carried out is shown in Figure 37. Notice that both forward transfer functions are modulated by the same square-wave function, $p_1(t)$. All linear transfer functions with nonrepeating roots can be expanded into partial fractions and treated in this way, even those transfer functions with numerator dynamics. Table III gives the closed form expressions for most elementary transfer function forms encountered in CN applications.

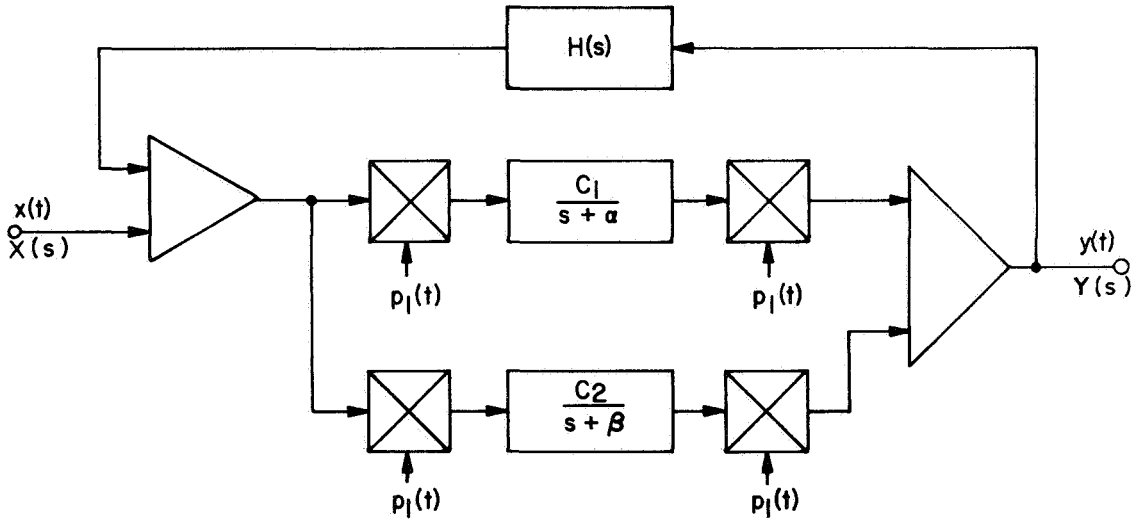

FIGURE 37. EQUIVALENT BLOCK DIAGRAM FOR THE PARTIAL FRACTION EXPANSION OF $G(s) = \frac{K}{(s + \alpha)(s + \beta)}$

The case for a forward transfer function with repeated roots is slightly more difficult to handle. To illustrate one method of treating repeated roots let

$$G(s) = \frac{K}{(\tau s + 1)^{\gamma}}, \tag{129}$$

where γ is a positive integer. Consider the case where $\gamma = 2$; then expression (123) can be written as

$$\sum_{\substack{\ell=-\infty \\ \text{odd}}}^{+\infty} \frac{K}{\ell(2r-\ell)(\tau s+1-j\ell\tau\omega_0)^2} \quad . \tag{130}$$

The closed form expression of equation (130) can be obtained by the theory of residues as presented by MacRobert [22]. The function that is integrated on a circle of infinite radius is

$$f(z) = \frac{K}{z(a-z)(b-cz)^2(1+e^{j\pi z})} \tag{131}$$

where

$$a = 2r$$

$$b = \tau s + 1$$

$$c = j\tau\omega_0 \ .$$

The last term in the denominator, $\frac{1}{1+e^{j\pi z}}$, has simple poles at the points $z = \pm 1, \pm 3, \pm 5, \ldots$, or all odd integers; the sum of its residues results in an expression similar to equation (130). The closed form expression for equation (130) is

$$\sum_{\substack{\ell=-\infty \\ \text{odd}}}^{+\infty} \frac{K}{\ell(2r-\ell)(\tau s+1-j\ell\tau\omega_0)^2} = -\frac{\pi^2 K\delta(r)}{4(\tau s+1)^2} - \frac{\pi^2 K \operatorname{sech}^2\frac{\pi}{2}\left(\frac{\tau s+1}{\tau\omega_0}\right)}{4(\tau s+1)(\tau s+1-j2r\tau\omega_0)}$$

$$+ \frac{\pi\tau\omega_0 K(\tau s+1-jr\tau\omega_0)}{(\tau s+1)^2(\tau s+1-j2r\tau\omega_0)^2} \tanh\frac{\pi}{2}\left(\frac{\tau s+1}{\tau\omega_0}\right), \tag{132}$$

where

$$\delta(r) = 1, \ r = 0$$

$$\delta(r) = 0, \ r \neq 0 \ .$$

The theory of residues can be used to sum infinite series that have terms higher than second-order in the denominator, but it is very unlikely that such terms will ever appear in any practical CN.

CONCLUSIONS

The most tractable method, of those investigated, for analyzing CN's employing full-wave balanced commutation was found to be Laplace transforms. When using Laplace transform techniques, a method has been developed for analyzing feedback systems employing CN's in the forward loop and any transfer function in the feedback loop. The method will handle any physically realizable transfer function used for the CN as well as any number of commutation phases. The method is applicable to both coupled and uncoupled CN's, and although it was developed for full-wave balanced CN's it is extendible to half-wave balanced CN's. It was shown that although CN's are linear from the superposition theory viewpoint, linear feedback theory is not applicable because of the harmonics present in the feedback loop.

Techniques for simplifying the analysis of CN's by the use of equivalent block diagrams are shown to provide additional insights into CN operation. For applications involving single-phase CN's, the importance of the phase relation between the input signal and that of the commutation function, when the input signal frequency equals the commutation function frequency, has been demonstrated by the quasi-continuous frequency response characteristic of the network.

A characteristic of CN's that may tend to limit their application is the generation of harmonics in the output signal. Polyphase CN's with properly phased commutation functions (more than two phases) are shown to simplify the harmonic suppression problem by increasing the order of the lowest harmonic present in the output signal.

The commutation function used for this investigation was the ideal square-wave. This is perhaps the most important of the commutation functions because it is easy and economical to mechanize. In the area of AC servo systems, however, one usually encounters sine wave modulation and demodulation functions. If square-wave CN's are used for compensation in an AC servo feedback system, the cascading of sine wave modulators with square-wave modulators will probably occur. Although the method developed for analyzing CN's with feedback

circuits can be used to obtain a useful approximate answer, it will not yield an exact solution to the AC servo feedback problem, nor will any other known method. This appears to be a good area for future study.

George C. Marshall Space Flight Center
National Aeronautics and Space Administration
Huntsville, Alabama, July 24, 1968
125-19-04-00-62

APPENDIX A
EXPERIMENTAL TEST EQUIPMENT AND PROCEDURES

To obtain frequency response data of the CN's investigated in this study, a frequency response analyzer, a Model 711A, Transfer Function Analyzer, made by Boonshaft and Fuchs, Incorporated, of Hatboro, Pennsylvania, was used. The analyzer consists of four functional units. The interconnection of these four units and that of the element under test are shown in block diagram form in Figure A-1. As shown in this figure, the analyzer consists of a low-frequency signal generator (LFG), a return signal analyzer (RSA), a phase and amplitude computer (PAC), and a timing interval reader (TIR). The external oscillator shown in Figure A-1 is used to drive the commutator units of the CN at the commutation frequency ω_0.

The Boonshaft Analyzer measures the frequency response over a range from 0.01 to 200 Hz with an accuracy of better than ± 2 degrees for phase and ± 0.25 dB for amplitude. The output data are presented as in-phase and quadrature components as well as total amplitude and phase. Noise on the return signal from the element under test is attenuated by 40 dB or more.

The LFG is mechanized as a second order loop that solves the differential equation of a sine wave using three chopper-stabilized operational amplifiers and two matched sets of precision condensers and resistors. An additional amplifier is used so that ± sin ωt and ± cos ωt signals are available for use in the RSA. An output amplifier provides the high power level output signal to drive the element under test. The frequency range of the LFG is from 0.0100 to 200 Hz, available in 5

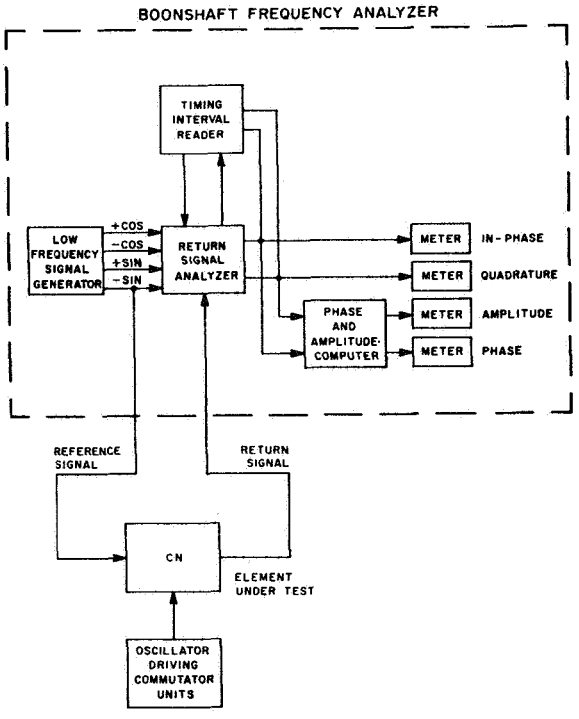

FIGURE A-1. BLOCK DIAGRAM OF FREQUENCY RESPONSE MEASUREMENTS

ranges. The frequency can be incremented by 0.001 of a unit for each frequency range with an accuracy of ± 1 percent of the setting. For the range 0.100 to 0.999 Hz, the increment can be as small as 0.001 Hz.

The RSA has two modes of operation, normal and fast. In the normal mode the RSA accepts the return signal from the element under test, performs a Fourier analysis, and separates it into in-phase and quadrature components. The Fourier analysis is accomplished by multiplying the return signal by the sine and cosine reference signals and averaging the results by passing them through low-pass filters. The resulting DC signals are directly proportional to the in-phase and quadrature components and are read-out on meters shown in Figure A-1.

The TIR contains a precision timing circuit for fast operation of the RSA on signal frequencies below 1.0 Hz. In the "fast" operate mode, the element under test is excited and then the unit is switched to operate and a precision timing circuit places the RSA into operation for 100 seconds in the 0.01 to 0.1 Hz frequency range and 10 seconds in the 0.1 to 1.0 Hz frequency range. The outputs from the multiplications in the RSA are integrated for a precise time interval and then the integrator is placed in a "hold" mode and the results are read out. The TIR also contains an offset meter and potentiometer for biasing out DC signals in the return signal up to ± 15 volts DC.

The PAC accepts the in-phase and quadrature signals from the RSA and computes the total amplitude and phase.

In taking the frequency response data of a single-capacitor CN, a slightly different procedure from that normally used had to be adopted to obtain good data. With an input signal frequency ω and a commutation frequency ω_0, the return signal to the RSA will contain frequency components ω, $2\omega_0 - \omega$, $2\omega_0 + \omega$, $4\omega_0 + \omega$, ... After multiplication by sin ωt, the output from the RSA will contain the frequencies 2ω, $2\omega_0$, $2\omega_0 - 2\omega$, $2\omega_0 + 2\omega$, . . . , plus a DC term. As the input signal frequency ω approaches ω_0, the $2\omega_0 - 2\omega$ frequency term becomes an extremely low frequency term and is not attenuated any appreciable amount. It is easy to visualize in the "fast" operation mode, how the output from the integrator would depend on where in the period of the $(2\omega_0 - 2\omega)$ component the integration stopped. To circumvent this potential source of error, the normal mode of operation was used and the DC component was obtained by averaging the high and low readings of the meters for both in-phase and quadrature components. The amplitude and phase were then hand calculated. With this procedure good agreement between theoretical and experimental data was obtained.

When the input signal frequency equaled the commutation frequency, the use of the separate oscillator to drive the commutator units was discontinued and the signal from the LFG was used to drive the commutator units. This procedure eliminated the possible error caused by drift in either oscillator and the difficult task of precisely matching the frequencies of two independent oscillators. It also permits a precise control of the phase between the input signal and commutation function.

APPENDIX B
SUMMATION FORMULAS

The following summation formulas, taken from Weiss [23] and Ryshik and Gradstein [24], are useful when analyzing CN:

$$\sum_{\substack{k=1 \\ \text{odd}}}^{\infty} \frac{1}{k^2 - x^2} = \frac{\pi}{4x} \tan \frac{\pi}{2} x \tag{B-1}$$

$$\sum_{\substack{k=1 \\ \text{odd}}}^{\infty} \frac{1}{k^2 + x^2} = \frac{\pi}{4x} \tanh \frac{\pi}{2} x \tag{B-2}$$

$$\sum_{\substack{k=1 \\ \text{odd}}}^{\infty} \frac{1}{(k^2 - x^2)(k^2 - y^2)} = \frac{\frac{\pi}{4x} \tan \frac{\pi}{2} x - \frac{\pi}{4y} \tan \frac{\pi}{2} y}{x^2 - y^2} \tag{B-3}$$

$$\sum_{\substack{k=1 \\ \text{odd}}}^{\infty} \frac{1}{(k^2 + x^2)(k^2 + y^2)} = \frac{\frac{\pi}{4x} \tanh \frac{\pi}{2} x - \frac{\pi}{4y} \tanh \frac{\pi}{2} y}{y^2 - x^2} \tag{B-4}$$

$$\sum_{\substack{k=1 \\ \text{odd}}}^{\infty} \frac{1}{(k^2 - x^2)(k^2 + y^2)} = \frac{\frac{\pi}{4} \tan \frac{\pi}{2} x - \frac{\pi}{4y} \tanh \frac{\pi}{2} y}{x^2 + y^2} \tag{B-5}$$

$$\sum_{\substack{k=1 \\ \text{odd}}}^{\infty} \frac{k^2}{(k^2 - x^2)(k^2 - y^2)} = \frac{\frac{\pi}{4}\left(x \tan \frac{\pi}{2} x - y \tan \frac{\pi}{2} y\right)}{x^2 - y^2} \tag{B-6}$$

$$\sum_{\substack{k=1 \\ \text{odd}}}^{\infty} \frac{k^2}{(k^2 + x^2)(k^2 + y^2)} = \frac{\frac{\pi}{4}\left(x \tanh \frac{\pi}{2}x - y \tanh \frac{\pi}{2}y\right)}{x^2 - y^2} \tag{B-7}$$

$$\sum_{\substack{k=1 \\ \text{odd}}}^{\infty} \frac{k^2}{(k^2 - x^2)(k^2 + y^2)} = \frac{\frac{\pi}{4}\left(x \tan \frac{\pi}{2}x + y \tanh \frac{\pi}{2}y\right)}{x^2 + y^2} \tag{B-8}$$

$$\sum_{k=1}^{\infty} \frac{1}{k^2 + x^2} = \frac{\pi}{2x} \coth \pi x - \frac{1}{2x^2} \tag{B-9}$$

$$\sum_{k=1}^{\infty} \frac{1}{k^2 - x^2} = \frac{1}{2x^2} - \frac{\pi \cot \pi x}{2x} \tag{B-10}$$

$$\sum_{k=1}^{\infty} \frac{1}{(2k - 1)^2} = \frac{\pi^2}{8} \tag{B-11}$$

$$\sum_{k=1}^{\infty} \frac{1}{(4k^2 - 1)^2} = \frac{\pi^2 - 8}{16} \tag{B-12}$$

REFERENCES

1. Borelli, M., and Hosenthien, H.: An Adaptive Tracking-Notch Filter for Suppression of Structural Bending Signals of Large Space Vehicles. NASA TM X-53,000, Oct. 1, 1963.

2. Hart, W., and McGowan, G.: An Advanced Control System for Saturn V Configuration, Phase I Final Report. NASA CR-63-24, Aug. 1963. (Confidential)

3. Borelli, M., Daniels, H., and Hosenthien, H.: Adaptive Tracking-Notch Filter System. Patent No. 3,375,451, March 26, 1968.

4. Hart, W., and McGowan, G.: An Advanced Control System for Saturn V Configuration, Phase IV Final Report, NASA CR-65-19, Jan. 1965. (Confidential)

5. Wilson, D.: Transfer Function of a Nonideal Chopper Demodulating Compensating Network. IEEE Trans. on Automatic Control, vol. AC-11, no. 2, Apr. 1966, pp. 326-327.

6. Ivey, K.: A-C Carrier Control Systems. Wiley & Sons, Inc., 1964.

7. Weiss, G.; Synchronous Networks. IRE Trans. on Automatic Control, vol. AC-7, Mar. 1962, pp. 42-49.

8. Le Page, W., Cahn, C., and Brown, J.: Analysis of a Comb Filter Using Synchronously Commutated Capacitors. AIEE Trans., Part I, 72, 1953, p. 63.

9. Smith, B.: Analysis of Commutated Networks. Trans. IRE, PGAE-10, p. 21.

10. Fischl, R.: Analysis of a Commutated Network. IEEE Trans. on Aerospace and Navigational Electronics, June 1963, pp. 114-123.

11. Franks, L. and Sandberg, I.: An Alternative Approach to the Realization of Network Transfer Functions: The N-Path Filter. Bell System Tech. J., Sept. 1960, pp. 1321-1350.

REFERENCES (Continued)

12. Tobin, B.: The Analysis and Synthesis of RC Synchronous Networks. PIB MRI-1016-62, Polytechnic Inst. of Brooklyn, June 5, 1962.

13. Asner, B.: Analysis of Notch Networks Containing Synchronously Commutated Capacitors of RC Combinations. NASA TN D-2625, Feb. 1965.

14. Feaster, W., Roan, F., Lowry, J., Chenoweth, D. and McDaniel, W.: An Analysis of An Adaptive Tracking Notch Filter. NAS8-1116, Dept. of Elec. Eng., Auburn Univ., Nov. 20, 1964.

15. Carroll, S.: Analytical Determination of Transfer Functions for RC Commutated Networks. NASA TN D-2948, Aug. 1965.

16. Tou, J., Weygandt, C., and Laveen, K.: Commutated Networks. Research Div. Rept. No. 58-12, Univ. of Pennsylvania, Aug. 31, 1957.

17. Roan, F.: Phase Stabilization of a Gyro Blender Using RC Commutated Networks. M.S. Thesis, Auburn Univ., Aug. 24, 1965.

18. Hosenthien, H.: Analysis of Carrier Systems by Modulation Equivalent Transfer Matrices. Army Ballistic Missile Agency, IR-10, Mar. 1, 1956.

19. Gardner, M. and Barnes, J.: Transients in Linear Systems. Ch. VIII, Wiley & Sons, Inc., 1949.

20. Hosenthien, H.: Modulation Equivalent Analysis. NASA: MSFC, Huntsville, Alabama (To be published as a NASA report).

21. Chen, W.: The Analysis of Linear Systems. Ch. IX, McGraw-Hill Book Co., Inc., 1963.

22. MacRobert, T.: Functions of a Complex Variable. Fourth Ed., Ch. VII, MacMillan & Co., Ltd., 1954.

REFERENCES (Concluded)

23. Weiss, G.: Chopper Network Analysis. Memorandum 5, R-708-58, PIB-636, Polytechnic Inst. of Brooklyn, Feb. 1959.

24. Ryshik, I., and Gradstein, I.: Tables of Series, Products and Integrals. Veb Deutscher Verlag der Wissenschaften, Berlin, 1936.

NASA-Langley, 1968 —— 10 M207

NATIONAL AERONAUTICS AND SPACE ADMINISTRATION
WASHINGTON, D.C. 20546
OFFICIAL BUSINESS

FIRST CLASS MAIL

POSTAGE AND FEES PAID
NATIONAL AERONAUTICS A
SPACE ADMINISTRATION

POSTMASTER: If Undeliverable (Section
Postal Manual) Do Not R

"The aeronautical and space activities of the United States shall be conducted so as to contribute . . . to the expansion of human knowledge of phenomena in the atmosphere and space. The Administration shall provide for the widest practicable and appropriate dissemination of information concerning its activities and the results thereof."

—NATIONAL AERONAUTICS AND SPACE ACT OF 1958

NASA SCIENTIFIC AND TECHNICAL PUBLICATIONS

TECHNICAL REPORTS: Scientific and technical information considered important, complete, and a lasting contribution to existing knowledge.

TECHNICAL NOTES: Information less broad in scope but nevertheless of importance as a contribution to existing knowledge.

TECHNICAL MEMORANDUMS: Information receiving limited distribution because of preliminary data, security classification, or other reasons.

CONTRACTOR REPORTS: Scientific and technical information generated under a NASA contract or grant and considered an important contribution to existing knowledge.

TECHNICAL TRANSLATIONS: Information published in a foreign language considered to merit NASA distribution in English.

SPECIAL PUBLICATIONS: Information derived from or of value to NASA activities. Publications include conference proceedings, monographs, data compilations, handbooks, sourcebooks, and special bibliographies.

TECHNOLOGY UTILIZATION PUBLICATIONS: Information on technology used by NASA that may be of particular interest in commercial and other non-aerospace applications. Publications include Tech Briefs, Technology Utilization Reports and Notes, and Technology Surveys.

Details on the availability of these publications may be obtained from:

SCIENTIFIC AND TECHNICAL INFORMATION DIVISION

NATIONAL AERONAUTICS AND SPACE ADMINISTRATION

Washington, D.C. 20546